TCAD simulations of innovative Low-Gain Avalanche Diodes for particle detector design and optimization

F. Moscatelli

On behalf of CNR-IOM, INFN and University of Perugia (Italy) and INFN and University of Torino (Italy) groups

This work has been supported by the Italian PRIN MIUR 2017 "4DInSiDe" research project and by the European Union's Horizon 2020 Research and Innovation programme under Grant Agreement No 101004761, AIDAinnova project.

Outline

- Motivations
- TCAD simulation of LGAD devices
  - Layout and doping profile
  - Physical models and parameters
- Methodology (DC, AC and transient response)
- Application of the developed model
  - Compensated LGAD
  - RSD LGAD

Outline

- Motivations
- TCAD simulation of LGAD devices
  - Layout and doping profile
  - Physical models and parameters
- Methodology (DC, AC and transient response)
- Application of the developed model
  - Compensated LGAD
  - RSD

Motivations

✓ **LGADs** are **n-in-p silicon** sensors
Operated in **low-gain regime** (20 – 30)
Critical electric field ~ 20 – 30 V/µm

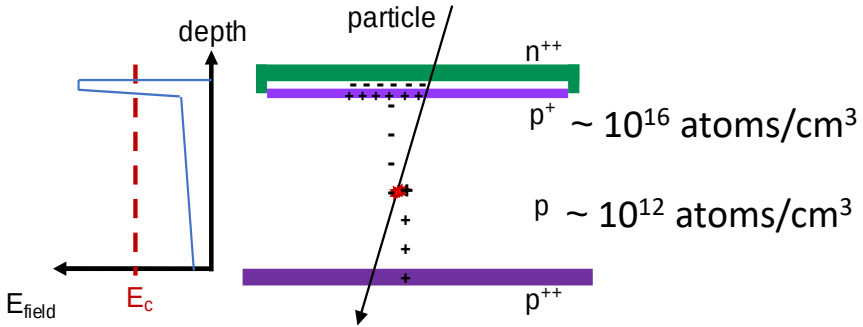

✓ The **acceptor removal mechanism**[1]
deactivates the p⁺-doping of the **gain layer** with irradiation

✓ **Device-level simulation tools**[2] **for predicting** the electrical behaviour and the charge collection properties **up to the highest particle fluences**.

✓ **Implementation** of a proper **radiation damage model** within the simulation environment.

[1] [M. Ferrero et al., doi:10.1016/j.nima.2018.11.121] **[2]** Synopsys© Sentaurus TCAD

Outline

- Motivations
- TCAD simulation of LGAD devices
  - Layout and doping profile
  - Physical models and parameters
- Methodology (DC, AC and transient response)
- Application of the developed model
  - Compensated LGAD
  - RSD

TCAD simulation of LGAD devices (1/2)

✓ **Layout** and **doping profile**

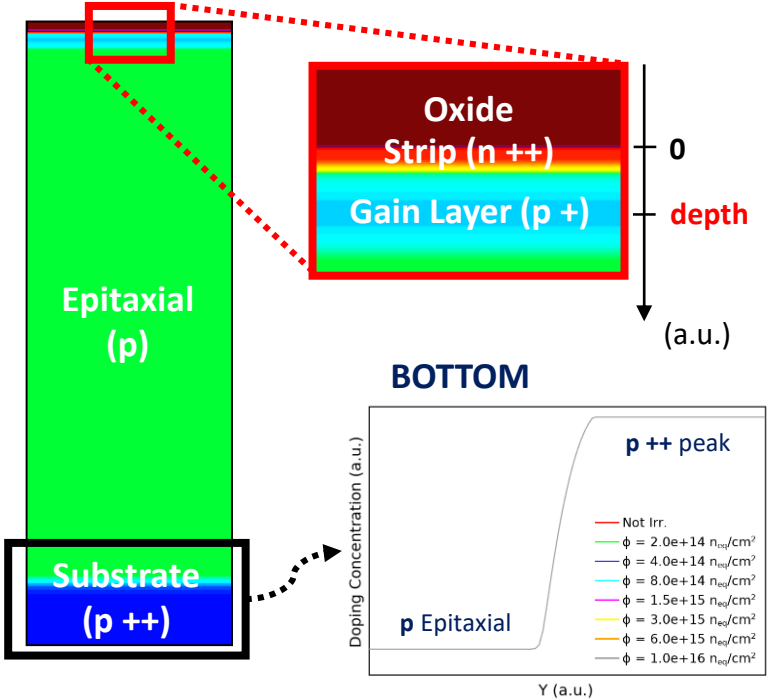

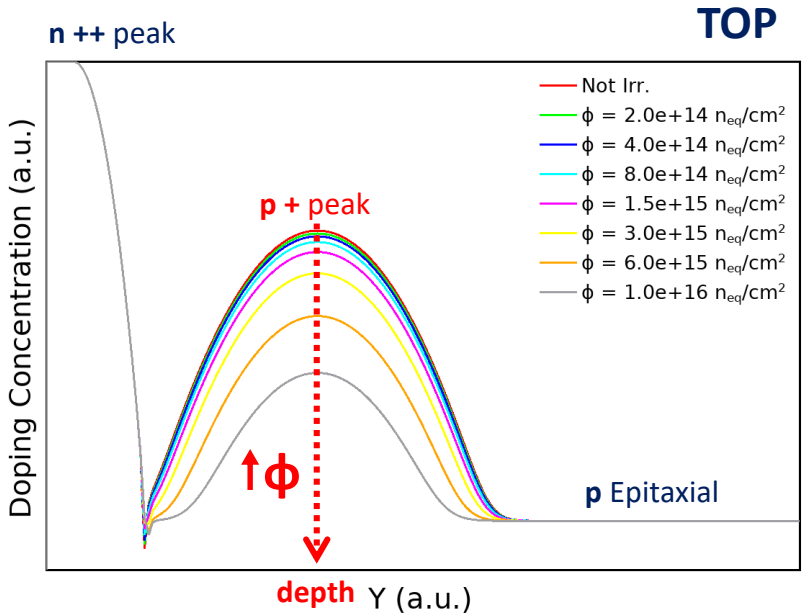

Gaussian Gain Layer **profile**

TCAD simulation of LGAD devices (2/2)

- ✓ Physical models
- ✓ **Generation/Recombination rate**
  - Shockley-Read-Hall, Band-To-Band Tunneling, Auger
  - **Avalanche Generation => impact ionization models**, such as *van Overstraeten-de Man*, *Okuto-Crowell*, *Massey*[2], *UniBo*
- ✓ **Fermi-Dirac statistics**
- ✓ **Carriers mobility variation** doping and field dependent
- ✓ **Physical parameters**
  - e-/h+ recombination lifetime
- ✓ Radiation damage models
- ✓ **"New University of Perugia model"**
  - **Combined surface and bulk** TCAD damage modelling scheme[3]
  - Traps generation mechanism
- ✓ **Acceptor removal mechanism** => $N_{GL}(\phi) = N_A(0)e^{-c\phi}$ where
  - **G**ain **L**ayer (**GL**)
  - **c**, removal rate, evaluated using the **Torino parameterization**[4]

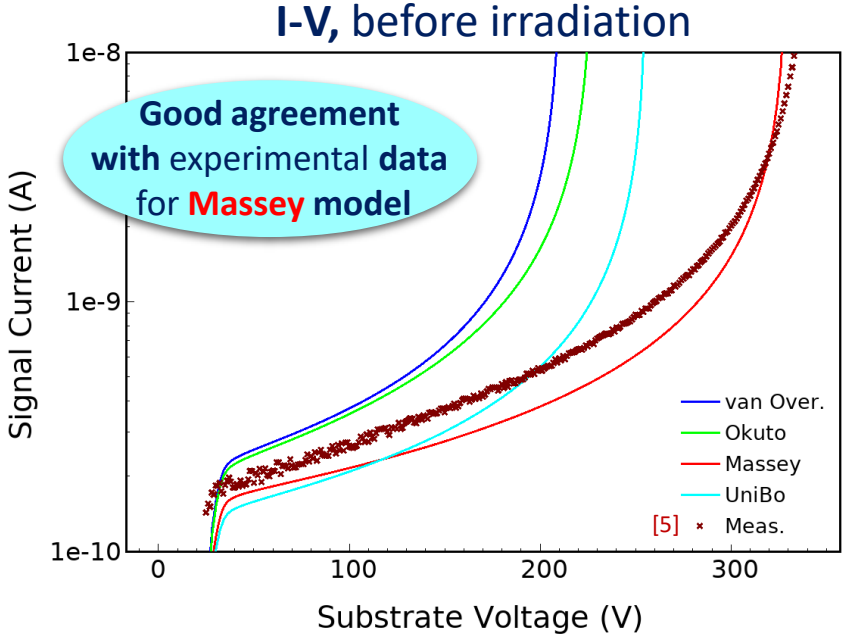

Temperature **300 K.** Electrical contact area **1mm²**

[2] M. Mandurrino et al., *Numerical Simulation of Charge Multiplication in Ultra-Fast Silicon Detectors (UFSD) and Comparison with Experimental Data*, IEEE, 2017.
[3] AIDA2020 report, *TCAD radiation damage model - CERN Document Server*.
[4] M. Ferrero et al., *Radiation resistant LGAD design*, Nucl. Inst. And Meth. In Phys. Res. A, November 30, 2018.
[5] V. Sola et al., *First FBK production of 50 µm ultra-fast silicon detectors*, Nucl. Instrum. Methods Phys. Res. A, 2019.

Outline

- Motivations
- TCAD simulation of LGAD devices
  - Layout and doping profile
  - Physical models and parameters
- Methodology (DC, AC and transient response)
- Application of the developed model
  - Compensated LGAD
  - RSD

Static (DC) and small-signal (AC) behavior

✓ **Comparison** with **experimental data**, **before** and **after irradiation**

Good agreement!

I-V

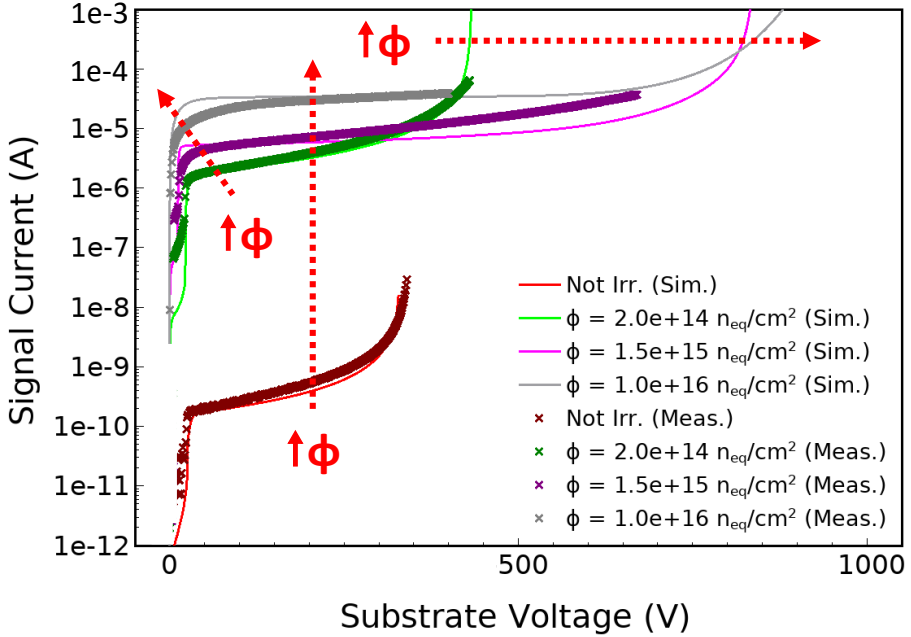

C-V

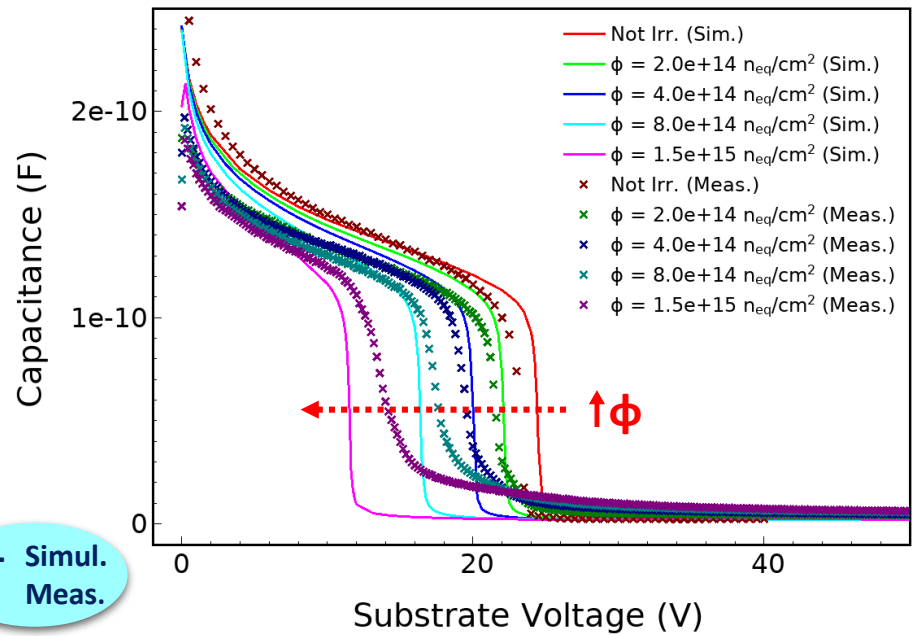

— Simul.
x Meas.

Avalanche model: **Massey**. Frequency **1 kHz** for **C-Vs**. Electrical contact area **1mm²**

[6] A. Chilingarov, *Temperature dependence of the current generated in si bulk*, JINST 8 P10003, 2013.

Transient response

✓ **Comparison** between **LGAD** and **PIN** response to the **MIP** for different V_{bias}

I-t, before irradiation

↑ϕ

I-t, fluence **1.5e15 n_{eq}/cm^2**

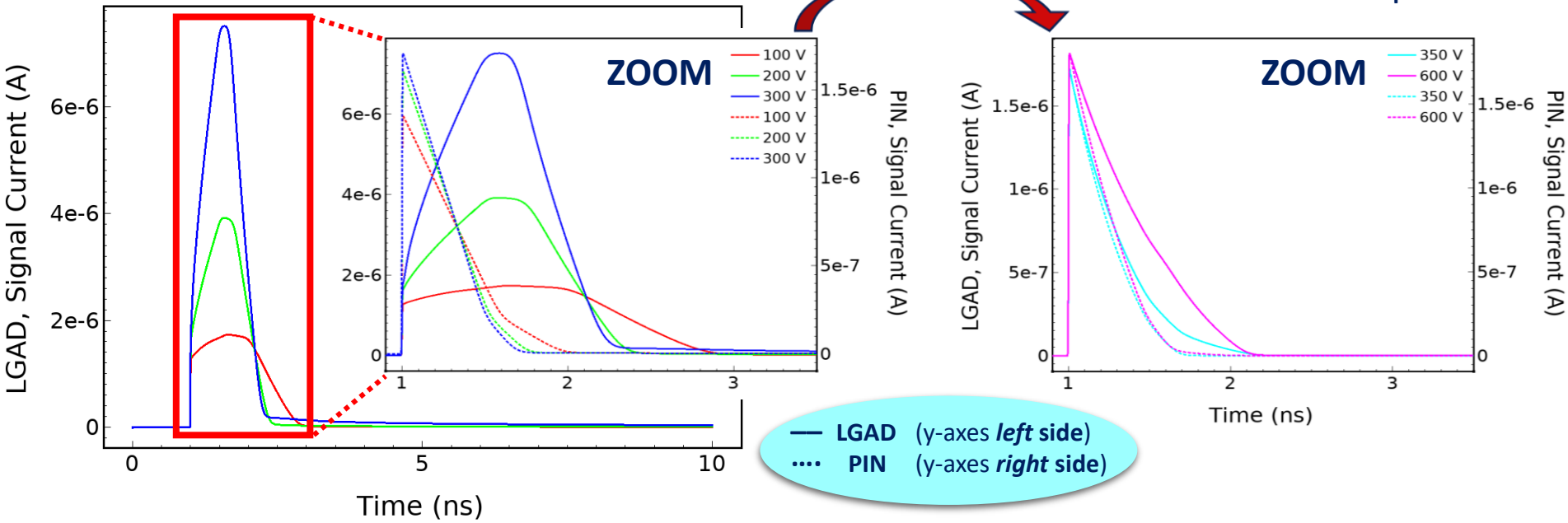

Avalanche model: **Massey**. Temperature **300 K**. Electrical contact area **1mm²**

[7] S. Meroli et al., *Energy loss measurement for charged particles in very thin silicon layers*, JINST 6 P06013, 2011.

Gain calculation

✓ Estimated **error** on **data ±10 %**

Good agreement!

G-V, before irradiation

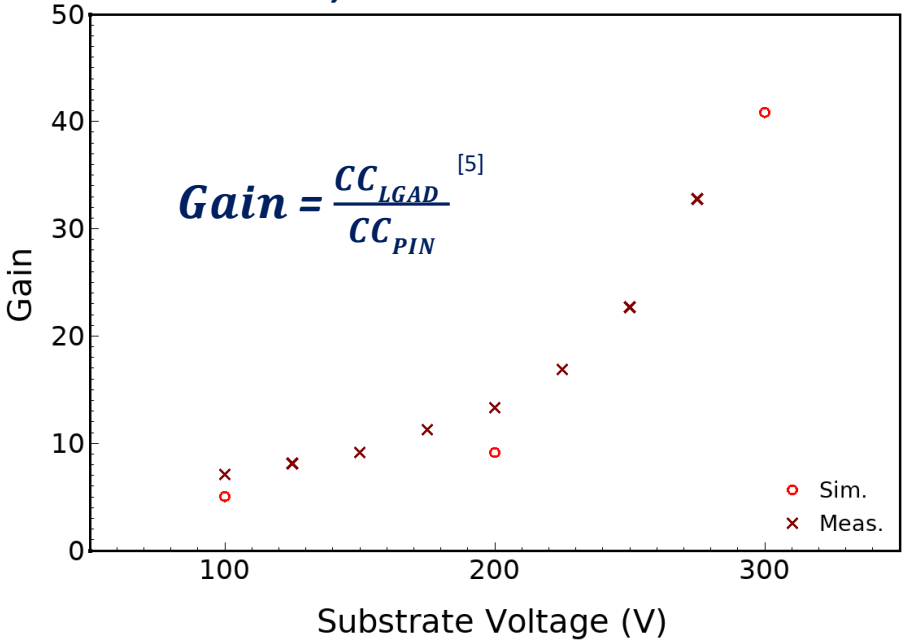

G-V, fluence **1.5e15 n_{eq}/cm^2**

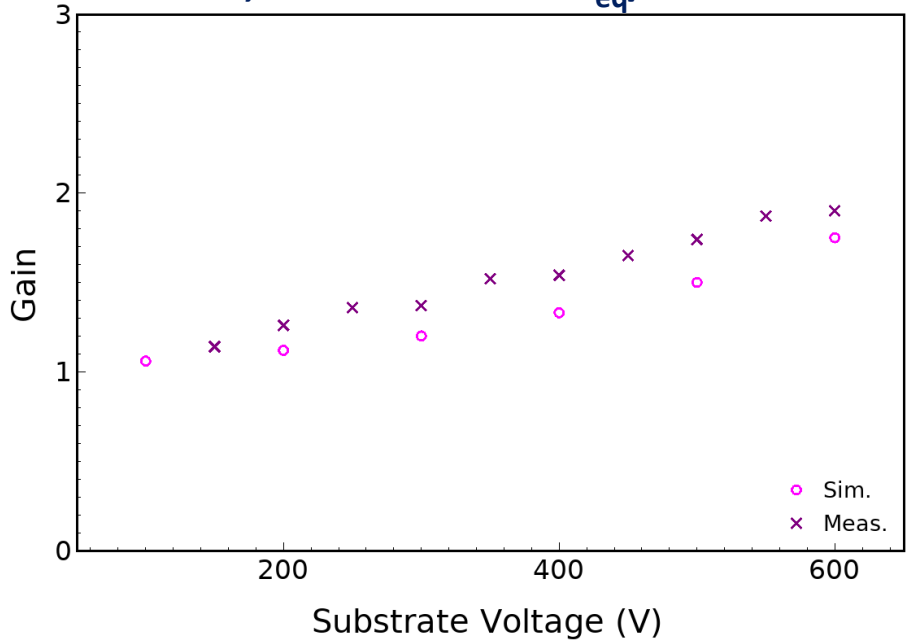

Avalanche model: **Massey**. Temperature **300 K**. Electrical contact area **1mm²**

[5] V. Sola et al., *First FBK production of 50 µm ultra-fast silicon detectors*, Nucl. Instrum. Methods Phys. Res. A, 2019.

Outline

- Motivations
- TCAD simulation of LGAD devices
  - Layout and doping profile
  - Physical models and parameters
- Methodology (DC, AC and transient response)
- Application of the developed model
  - Compensated LGAD
  - RSD

LGAD for extreme fluences

✓ **Difficult to operate silicon sensors above 10^{16} n_{eq}/cm^2 due to**:

– defects in the silicon lattice structure → increase of the dark current

– trapping of the charge carriers → decrease of the charge collection efficiency

– change in the bulk effective doping → impossible to fully deplete the sensors

- For LGAD acceptor removal mechanism

✓ **The options to overcome the present limits above 10^{16} n_{eq}/cm^2 are:**

1. **saturation** of the radiation damage effects above $5 \cdot 10^{15}$ n_{eq}/cm^2
2. the use of **thin** active substrates (20 – 40 μm)
3. **extension** of the charge carrier multiplication up to 10^{17} n_{eq}/cm^2

Towards a Radiation Resistance Design

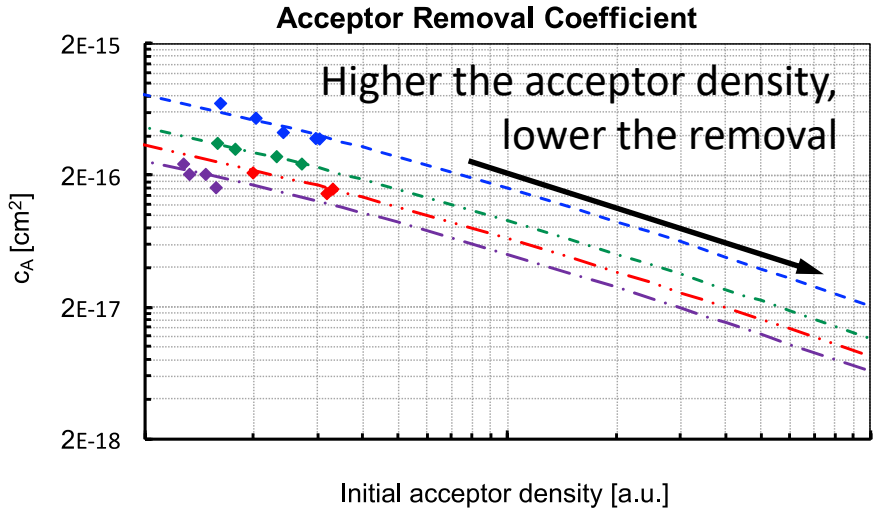

The acceptor removal mechanism deactivates the p^+-doping of the **gain layer** with irradiation according to

$$p^+(\Phi) = p^+(0)\cdot e^{-c_A\Phi}$$

where c_A is the acceptor removal coefficient

c_A depends on the initial acceptor density, $p^+(0)$, and on the defect engineering of the gain layer atoms

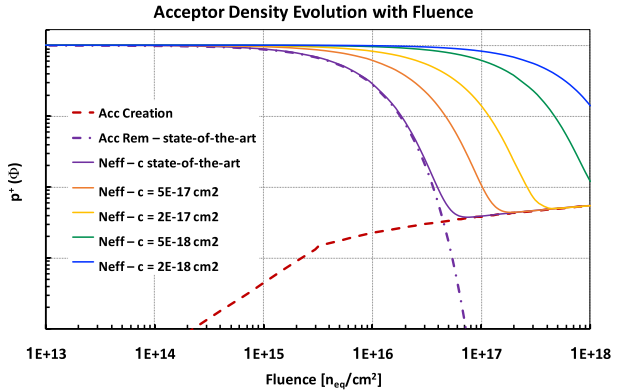

Lowering c_A extends the gain layer survival up to the highest fluences

Compensation

Impossible to reach the design target with the present design of the gain layer

Use the interplay between acceptor and donor removal to keep a constant gain layer active doping density

Many unknown:

- donor removal coefficient, from $n^+(\Phi) = n^+(0)\cdot e^{-cD\Phi}$
- interplay between donor and acceptor removal (c_D vs c_A)
- effects of substrate impurities on the removal coefficients

V. Sola et al, "A compensated design of the LGAD gain layer», NIMA 1040 (2022) 167232

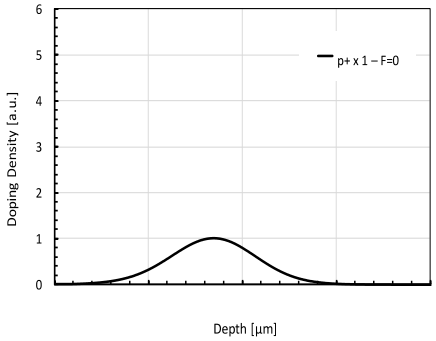

Standard LGAD design

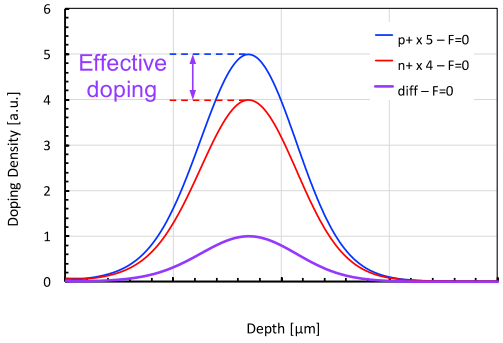

Compensated LGAD

Compensation – doping evolution with fluence

Three scenarios of net doping evolution with fluence are possible, according to the acceptor and donor removal interplay :

1. $c_A \sim c_D$

   p^+ & n^+ difference will remain constant ⇒ unchanged gain with irradiation

   → **This is the best possible outcome**

2. $c_A > c_D$

   effective doping disappearance is slower than in the standard design

   → **Co-implantation of Carbon** atoms mitigates the removal of p^+-doping

3. $c_A < c_D$

   n^+-atoms removal is faster ⇒ increase of the gain with irradiation

   → **Co-implantation of Oxygen** atoms might mitigate the removal of n^+-doping

Compensation - simulation

Process simulations of Boron (p^+) and Phosphorus (n^+) implantation and activation reveal the different shape of the two profiles (TCAD Silvaco)

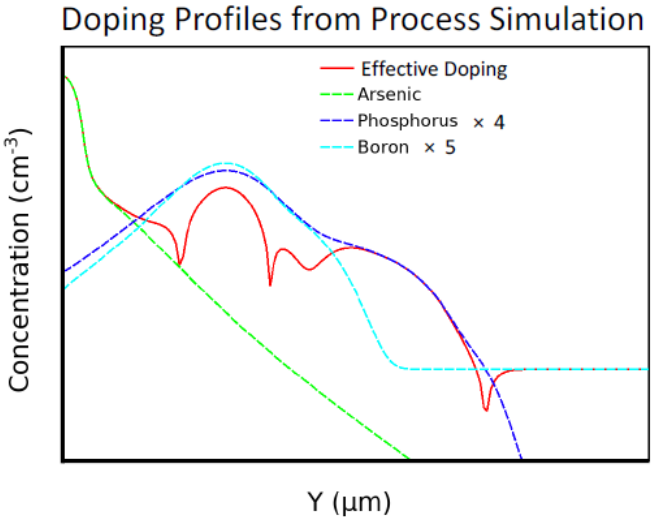

Compensation - simulation

Process simulations of Boron (p^+) and Phosphorus (n^+) implantation and activation reveal the different shape of the two profiles (TCAD Silvaco)

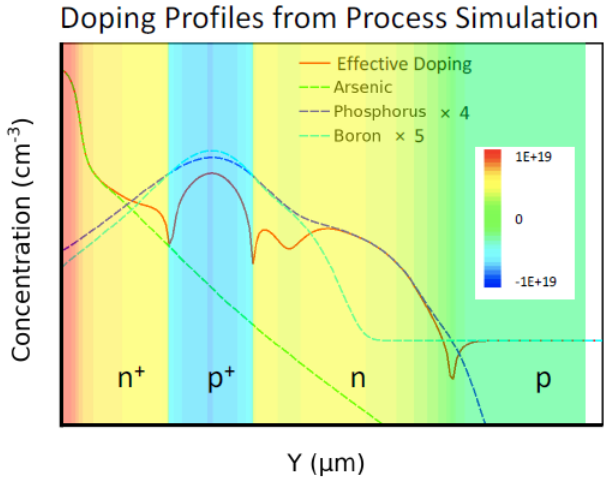

Difficult to precisely control the interplay between the implanted p^+ and n^+ densities

Compensation - simulation

Process simulations of Boron (p^+) and Phosphorus (n^+) implantation and activation reveal the different shape of the two profiles (TCAD Silvaco)

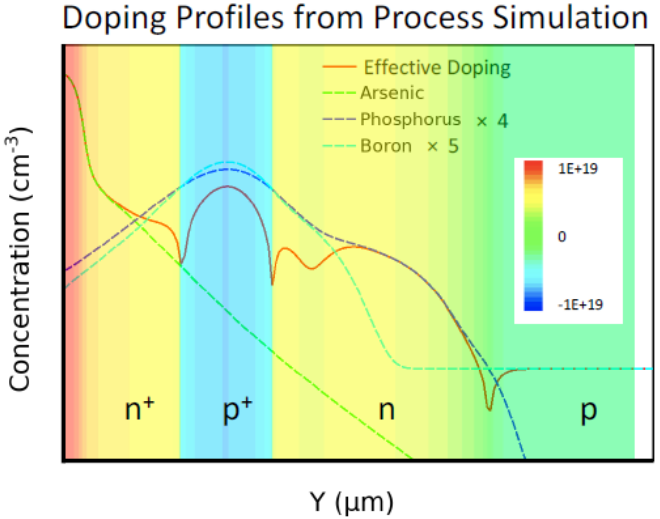

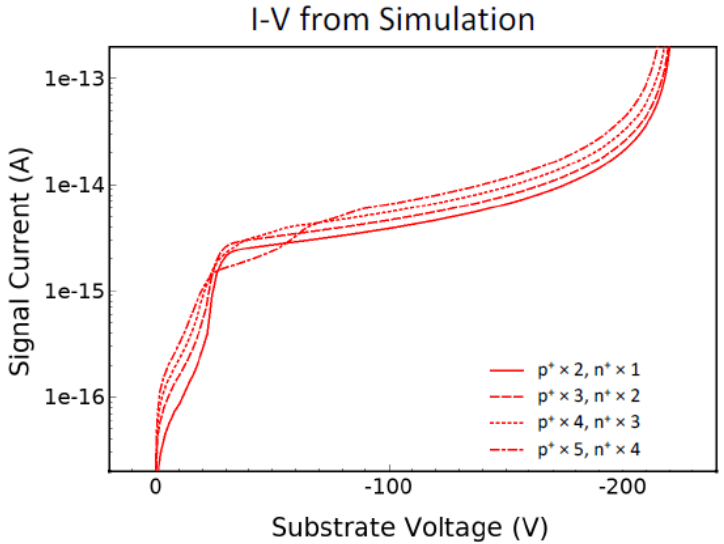

→ The simulation of the electrostatic behaviour show that it is possible to reach similar multiplication for different values of initial compensation (TCAD Synopsys)

Outline

- Motivations
- TCAD simulation of LGAD devices
  - Layout and doping profile
  - Physical models and parameters
- Methodology (DC, AC and transient response)
- Application of the developed model
  - Compensated LGAD
  - RSD

RSD and DC-RSD

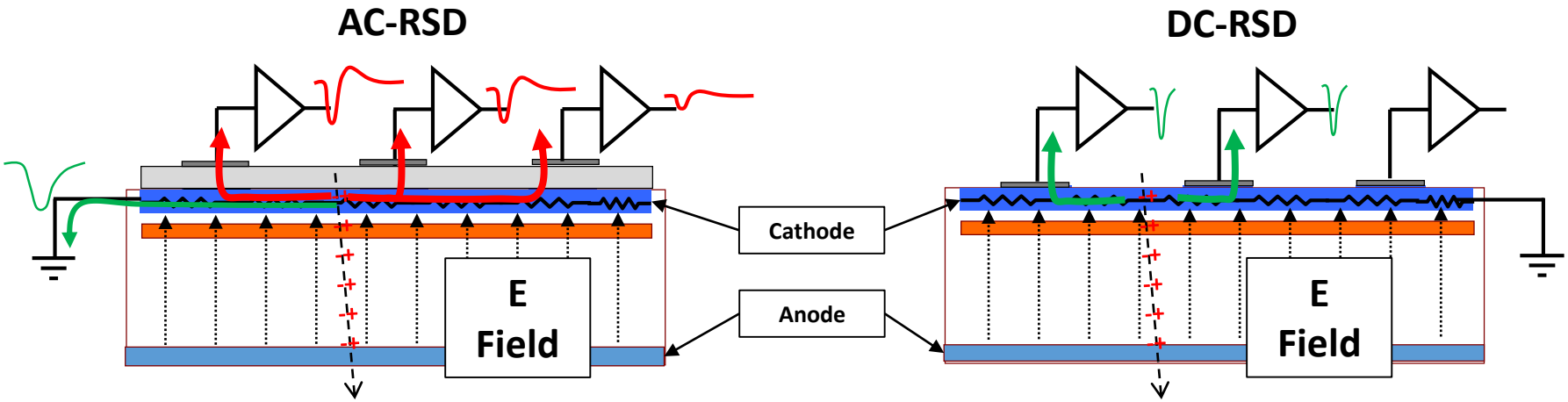

This design has been manufactured in several productions by FBK, BNL, and HPK

This design is presently under development by FBK

The main advantage of the DC-RSD design is to limit the signal spread

Simulated layout

✓ **3D** structure, **2x2 PADs**

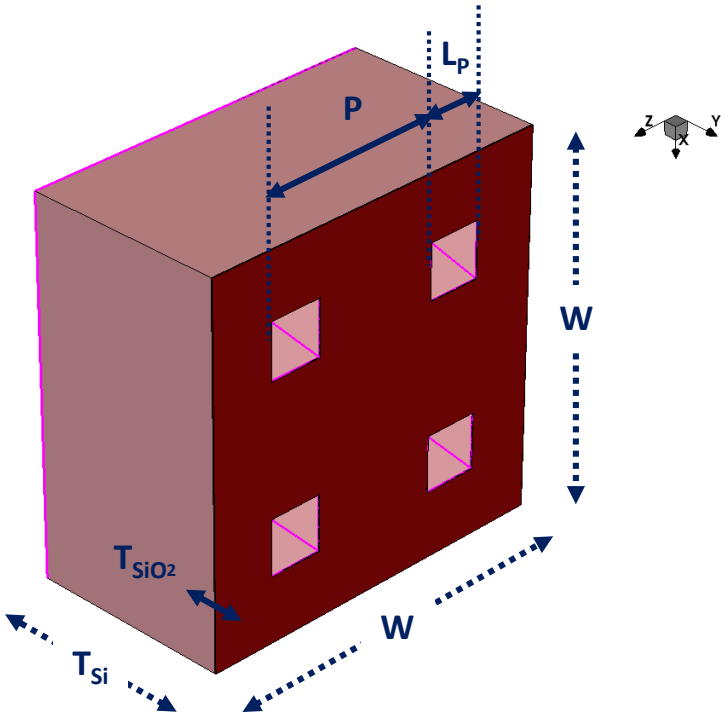

- ✓ **Silicon (Si)**
  - Width (W) 100 µm
  - Thickness (T) 55 µm
- ✓ **Silicon Oxide (SiO_2)**
  - Width (W) 100 µm
  - Pad Length (L_P) **15 µm**
  - Pitch (P) **50 µm**
  - Thickness (T) 0,30 µm

Active (TV) behavior (1/2)

- ✓ **3D** structure, **2x2 PADs**
  - **hit 1** (center hit), **1 MIP**
  - V_s = **-200 V**

@ $R_{s,n++} \approx 203\ \Omega_{sq}$

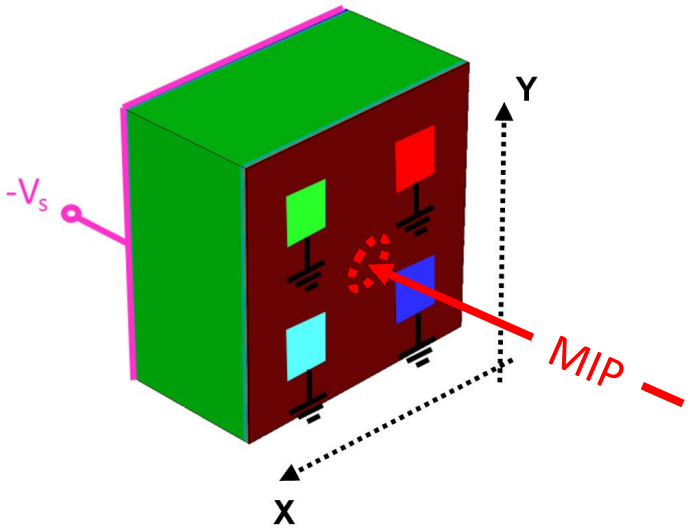

I-t, not irr.

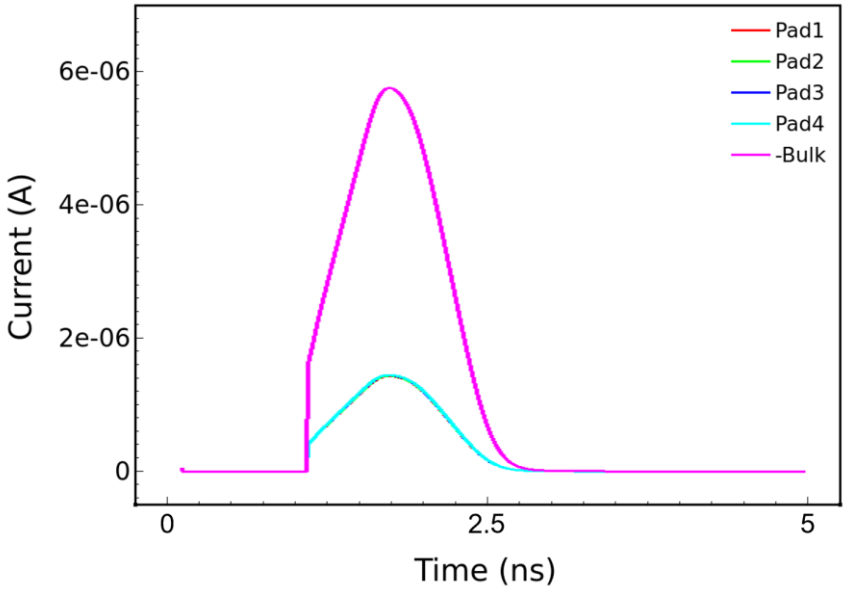

Avalanche model: **Massey**. Temperature **300 K**

Active (TV) behavior (2/2)

- ✓ **3D** structure, **2x2 PADs**
  - **hit 2**, **1 MIP**
  - V_s = **-200 V**

@ $R_{s,n++} \approx 203\ \Omega_{sq}$

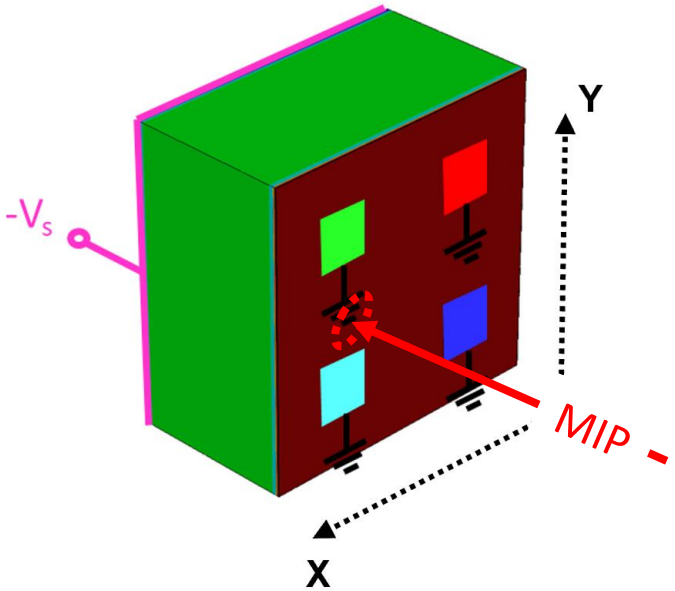

I-t, not irr.

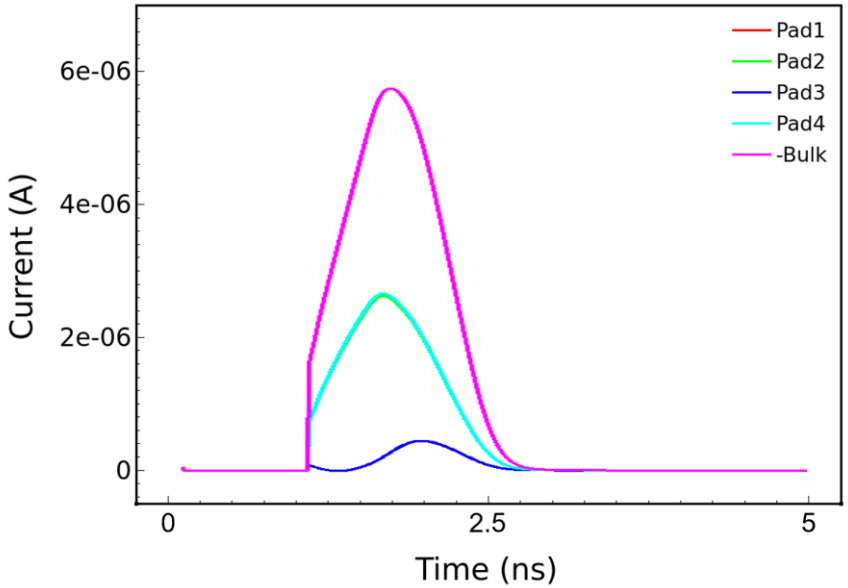

Avalanche model: **Massey**. Temperature **300 K**

Different n^{++} layer resistance

✓ **3D** structure, **2x2 PADs** => **LGAD**

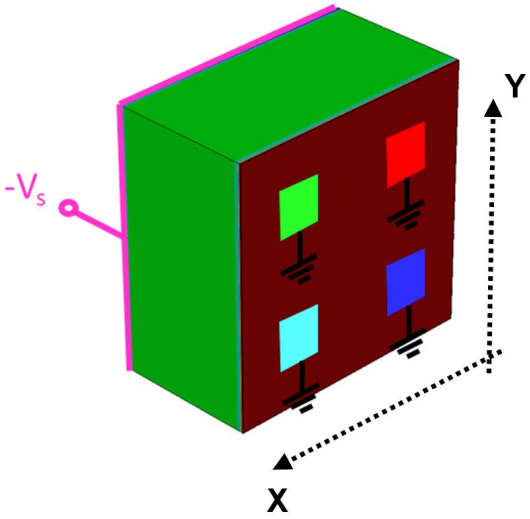

I-V, not irr.

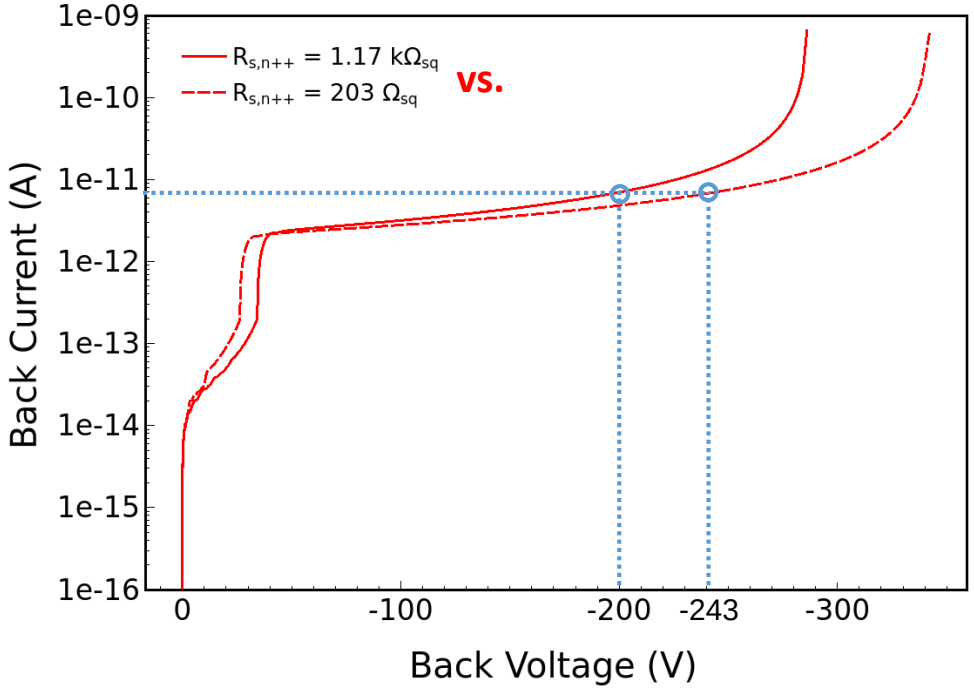

Avalanche model: **Massey**. Temperature **300 K**

Different n^{++} layer resistance: Active behavior

- ✓ **3D** structure, **2x2 PADs** => **LGAD**
  - **hit 1** (center hit), **1 MIP**
  - V_s = **-243 V** ---> V_s = **-200 V**

$R_{s,n++} \approx 203\ \Omega_{sq}$ ---> $R_{s,n++} \approx 1{,}17\ k\Omega_{sq}$

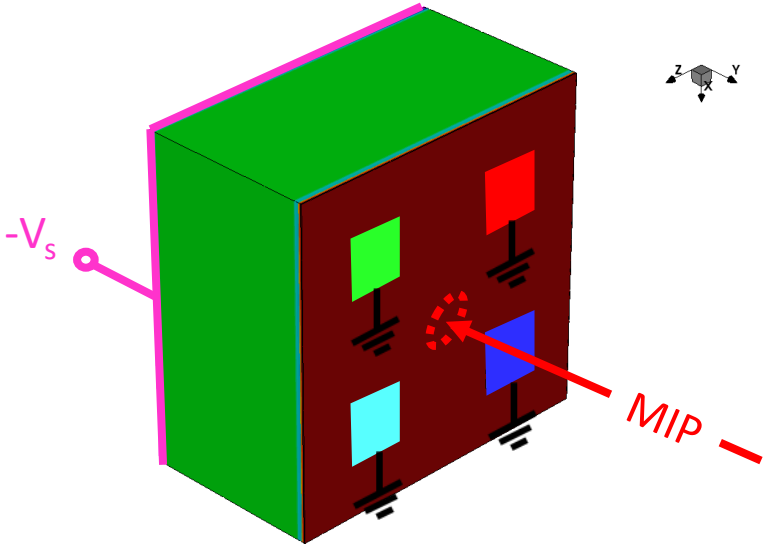

I-t, not irr. (ZOOM)

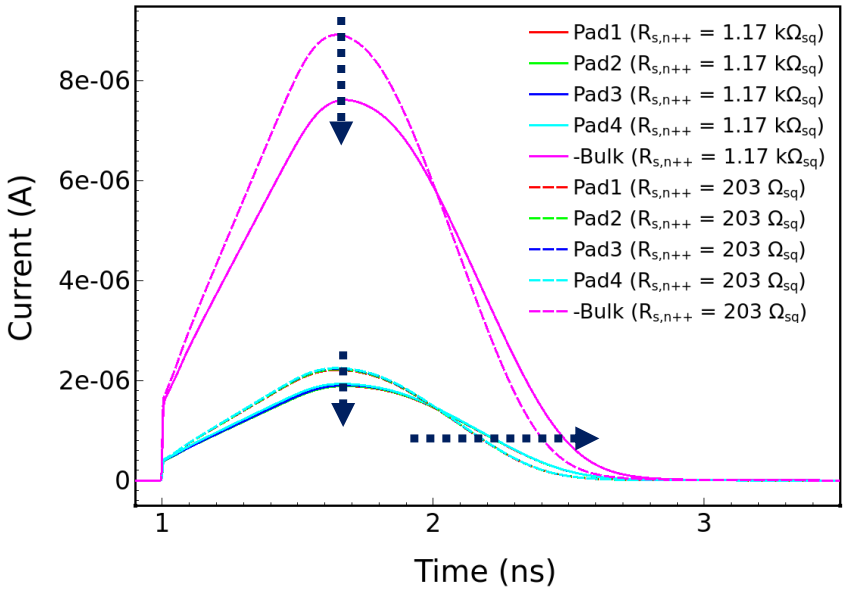

Avalanche model: **Massey**. Temperature **300 K**

Different n^{++} layer resistance: Active (TV) behavior

- ✓ **3D** structure, **2x2 PADs** => **LGAD**
  - **hit 3**, **1 MIP**
  - V_s = -243 V ---> V_s = -200 V

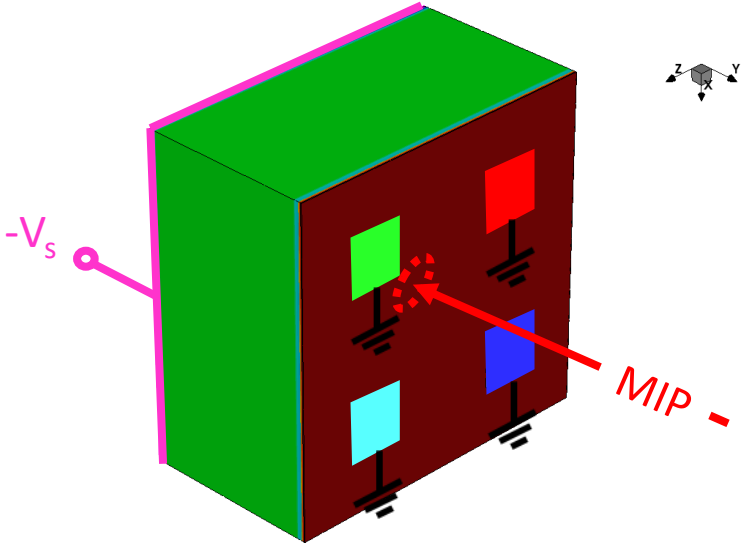

$R_{s,n++} \approx 203\ \Omega_{sq}$ ---> $R_{s,n++} \approx 1{,}17\ k\Omega_{sq}$

I-t, not irr. (ZOOM)

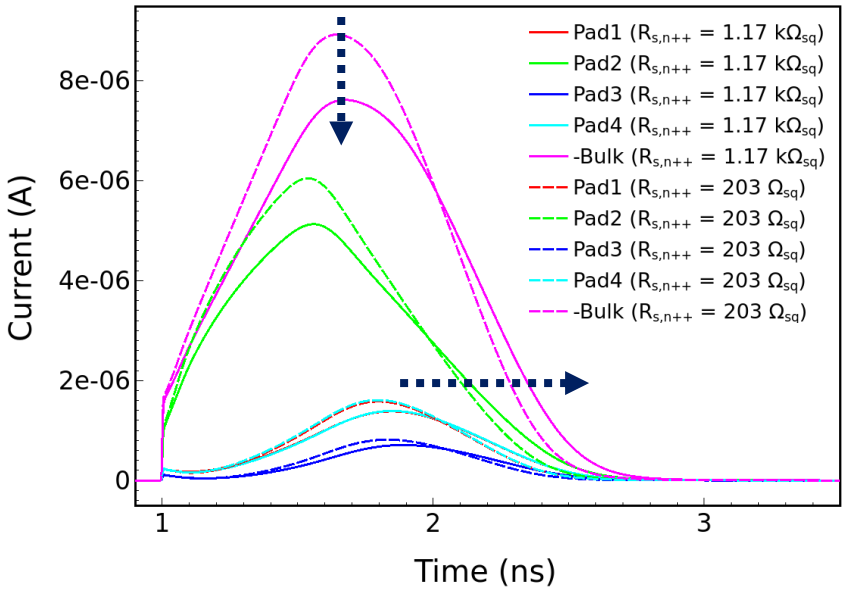

Avalanche model: **Massey**. Temperature **300 K**

Reconstruction (1/2)

✓ The position is reconstructed using the **CHARGE imbalance**

$$x_i = \frac{Q_{top\,right} + Q_{bottom\,right} - Q_{top\,left} - Q_{bottom\,left}}{Q_{tot}}$$

$$z_i = \frac{Q_{top\,right} + Q_{top\,left} - Q_{bottom\,left} - Q_{bottom\,right}}{Q_{tot}}$$

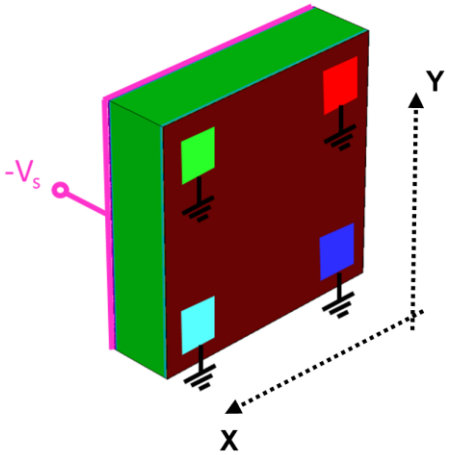

Thickness = 40 µm

Pad Length = 15 µm

Pitch = 105 µm

@ V_{Back} = -110 V

1 MIP

$R_{s,n++} \approx 721\ \Omega_{sq}$

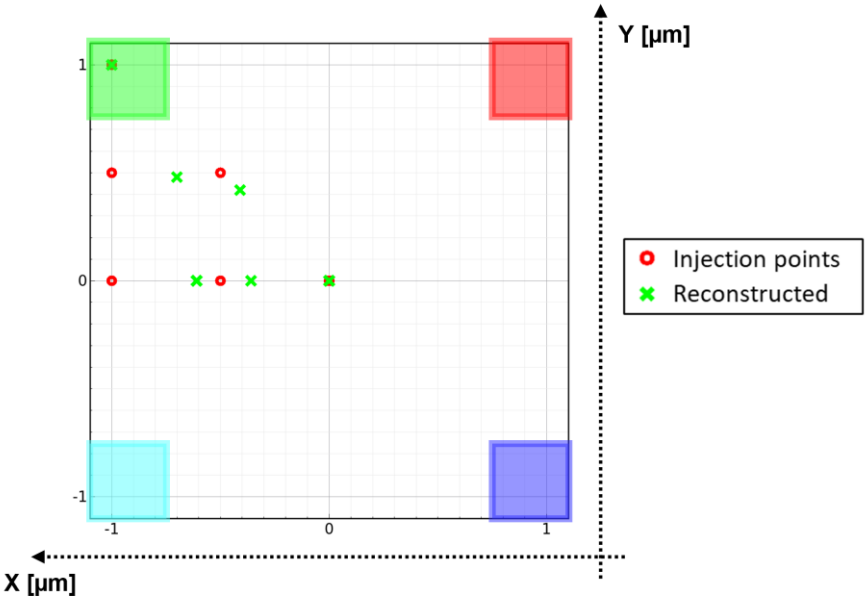

Results from *TCAD* simulations

Avalanche model: **Massey**. Temperature **300 K**

Reconstruction (2/2)

✓ The position is reconstructed using the **CHARGE imbalance**

$$x_i = \frac{Q_{top\,right} + Q_{bottom\,right} - Q_{top\,left} - Q_{bottom\,left}}{Q_{tot}}$$

$$z_i = \frac{Q_{top\,right} + Q_{top\,left} - Q_{bottom\,left} - Q_{bottom\,right}}{Q_{tot}}$$

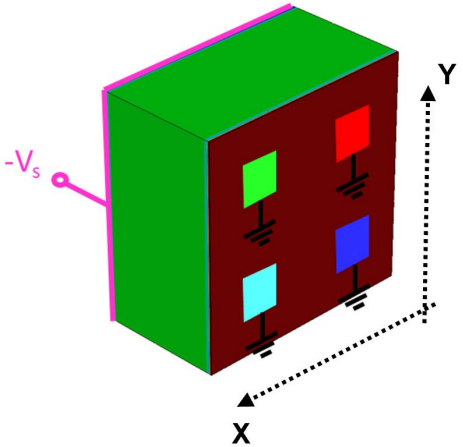

Thickness = 55 µm

Pad Length = 15 µm

Pitch = 50 µm

@ V_{Back} = -200 V

1 MIP

$R_{s,n++} \approx 203\ \Omega_{sq}$

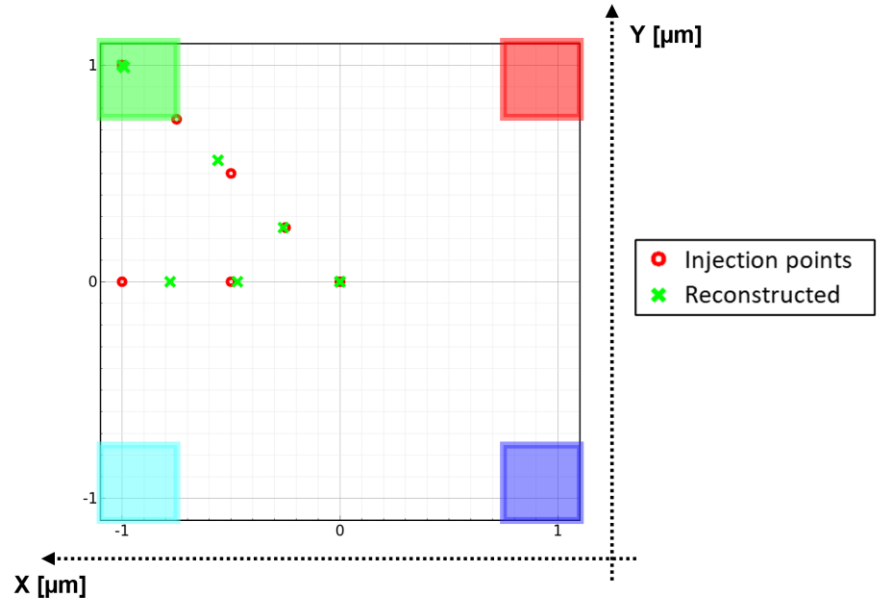

Results from *TCAD* simulations

Avalanche model: **Massey**. Temperature **300 K**

DC-RSD with resistors

The DC-RSD design can also be done **including resistors** between the read-out electrodes.

these resistors could improve the position resolution of the sensors

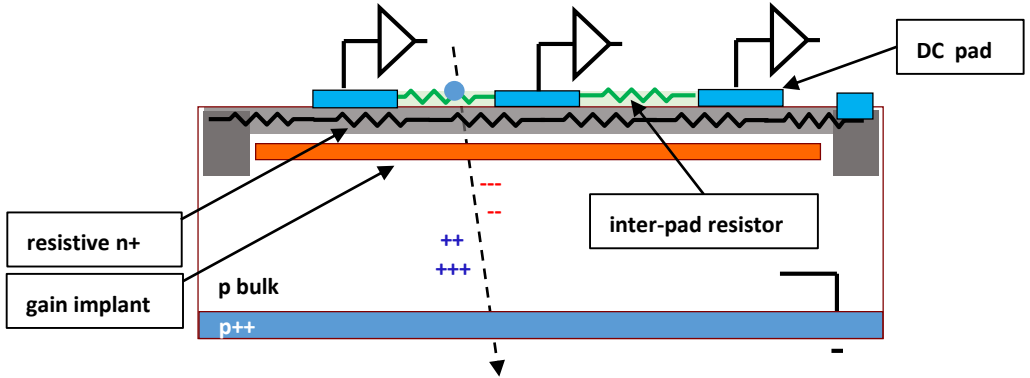

RSD with resistors between read-out electrodes

✓ **3D** structure, **2x2 PADs** => **LGAD**

@ $R_{s,n++} \approx 721\ \Omega_{sq}$

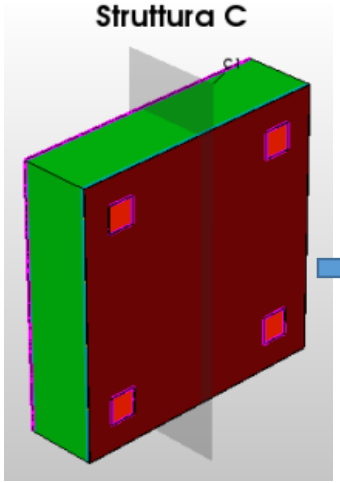

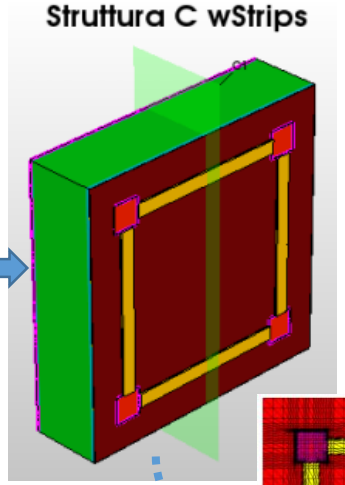

287.514 mesh points

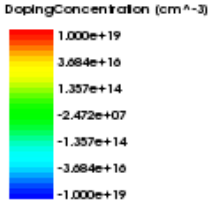

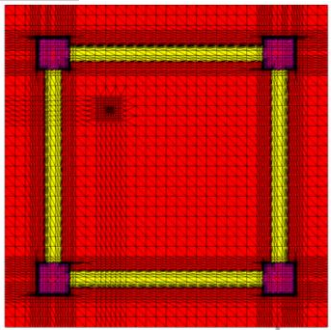

351.889 mesh points

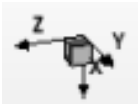

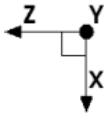

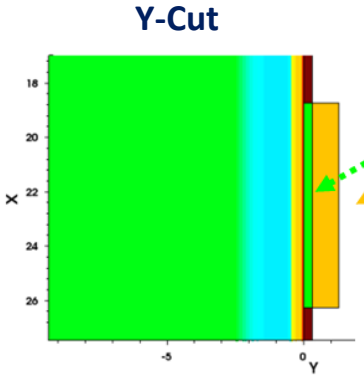

TiTiN

R_{TiTiN}

3,06 Ω/µm
490 mΩ/µm
228 mΩ/µm
15 mΩ/µm

Active (TV) behavior (1/2)

- ✓ **3D** structure, **2x2 PADs**, type C **w Strip**
  - **hit 3**, **1 MIP**
  - **V_s = -110 V**

@ $R_{s,n++} \approx 721\ \Omega_{sq}$

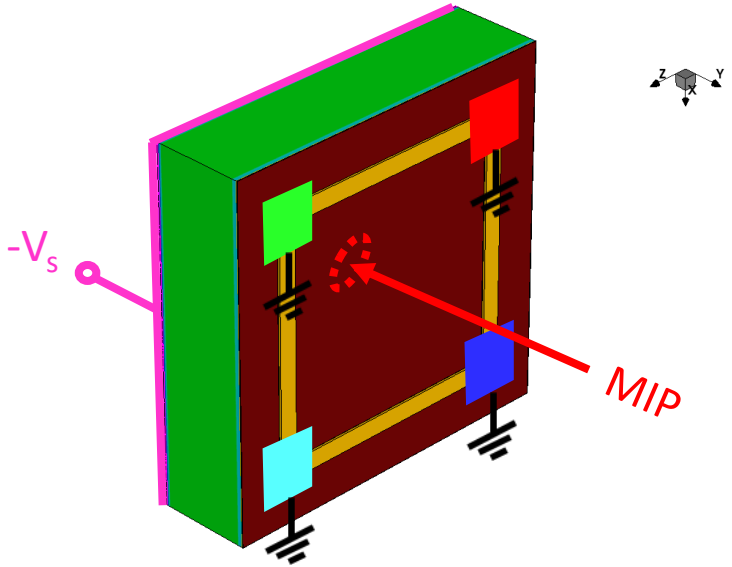

I-t, not irr. (ZOOM)

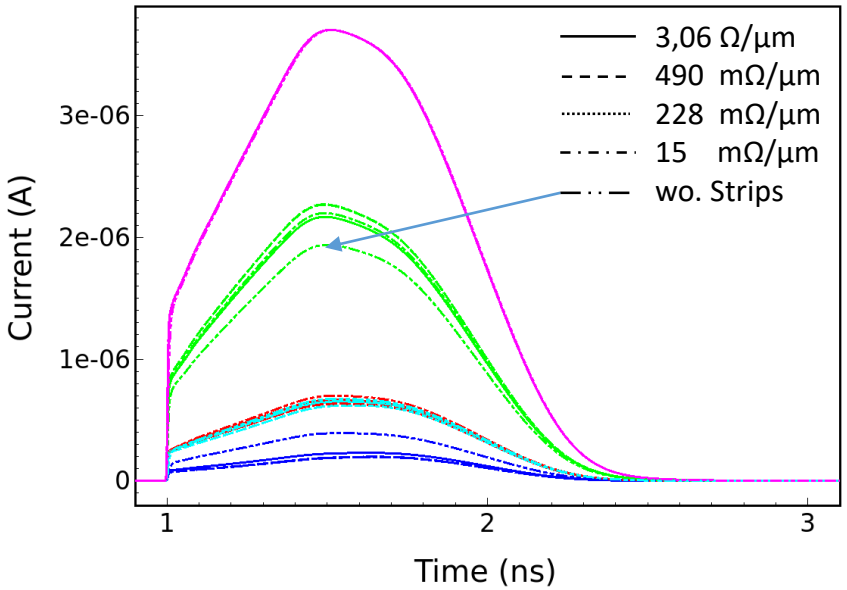

Avalanche model: **Massey**. Temperature **300 K**

Active (TV) behavior (2/2)

- ✓ **3D** structure, **2x2 PADs**, type C **w Strip**
  - **hit 8**, **1 MIP**
  - **V_s = -110 V**

@ $R_{s,n++} \approx 721\ \Omega_{sq}$

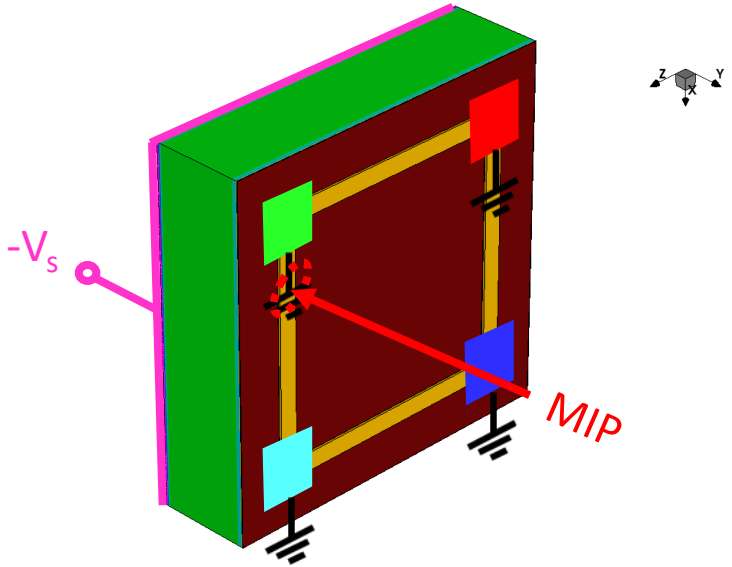

I-t, not irr. (ZOOM)

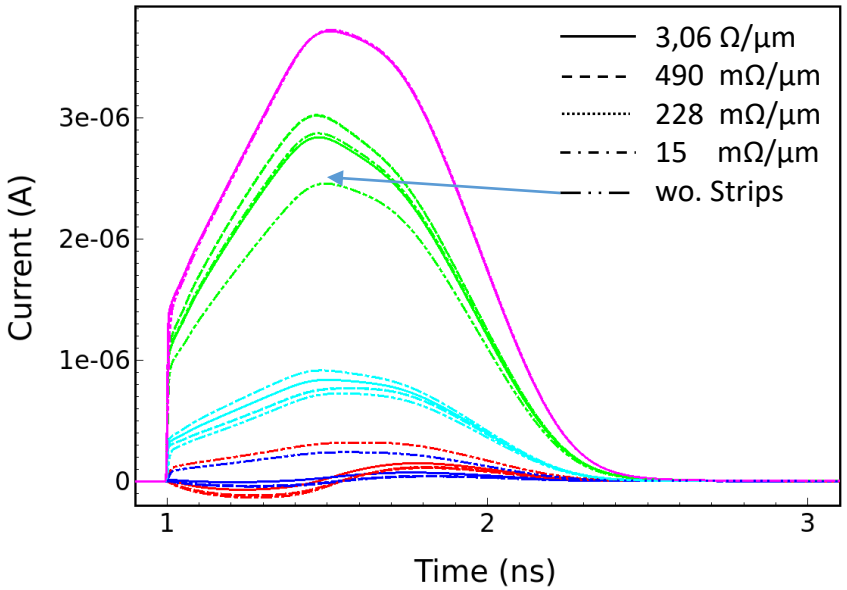

Avalanche model: **Massey**. Temperature **300 K**

Reconstruction with strips

✓ The position is reconstructed using the **CHARGE imbalance**

$$x_i = \frac{Q_{top\,right} + Q_{bottom\,right} - Q_{top\,left} - Q_{bottom\,left}}{Q_{tot}}$$

$$z_i = \frac{Q_{top\,right} + Q_{top\,left} - Q_{bottom\,left} - Q_{bottom\,right}}{Q_{tot}}$$

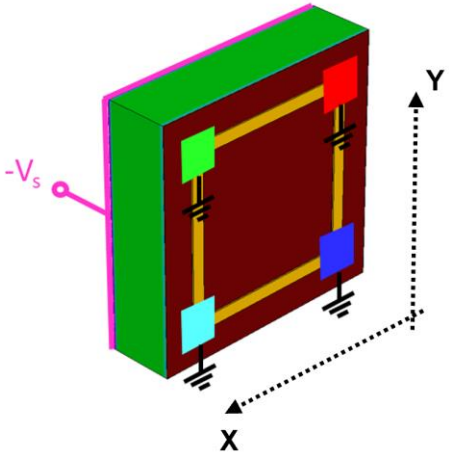

Pad Length = 15 µm

Pitch = 105 µm

@ V_{Back} = -110 V

1 MIP

$R_{s,n++} \approx 721\ \Omega_{sq}$

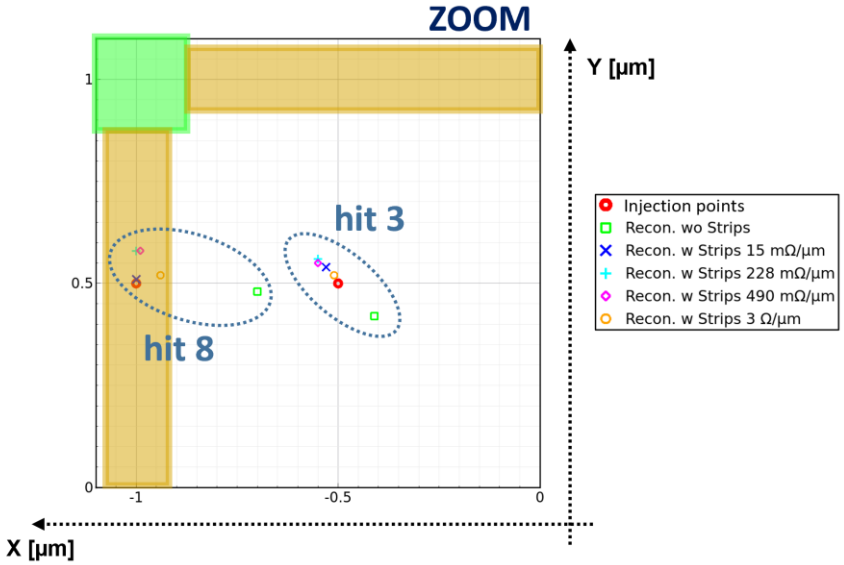

Results from *TCAD* simulations

Avalanche model: **Massey**. Temperature **300 K**

Reconstruction with strips

✓ The position is reconstructed using the **CHARGE imbalance**

$$x_i = \frac{Q_{top\,right} + Q_{bottom\,right} - Q_{top\,left} - Q_{bottom\,left}}{Q_{tot}}$$

$$z_i = \frac{Q_{top\,right} + Q_{top\,left} - Q_{bottom\,left} - Q_{bottom\,right}}{Q_{tot}}$$

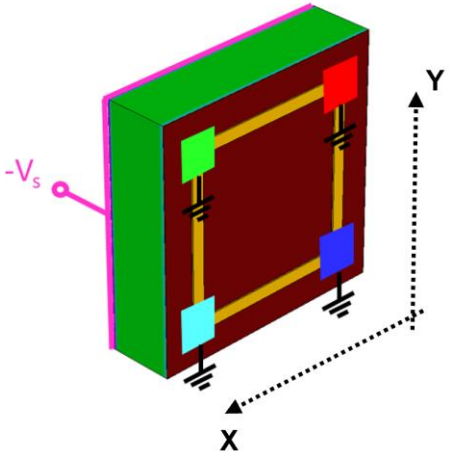

Pad Length = 15 µm

Pitch = 105 µm

@ V_{Back} = -110 V

1 MIP

$R_{s,n++} \approx 721\ \Omega_{sq}$

$R_{s,strip} \approx 15\ m\Omega/\mu m$

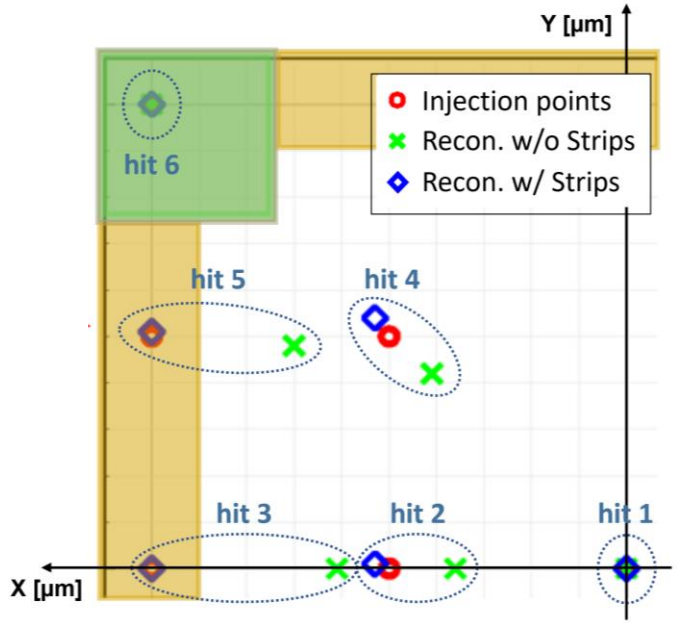

Results from *TCAD* simulations

Avalanche model: **Massey**. Temperature **300 K**

Impact of the pad size

✓ **3D** structure, **2x2 PADs** => **LGAD**

@ $R_{s,n++} \approx 721\ \Omega_{sq}$

L_{PAD} **= 15 µm** => pitch = 105 µm

L_{PAD} **= 7 µm** => pitch = 109 µm

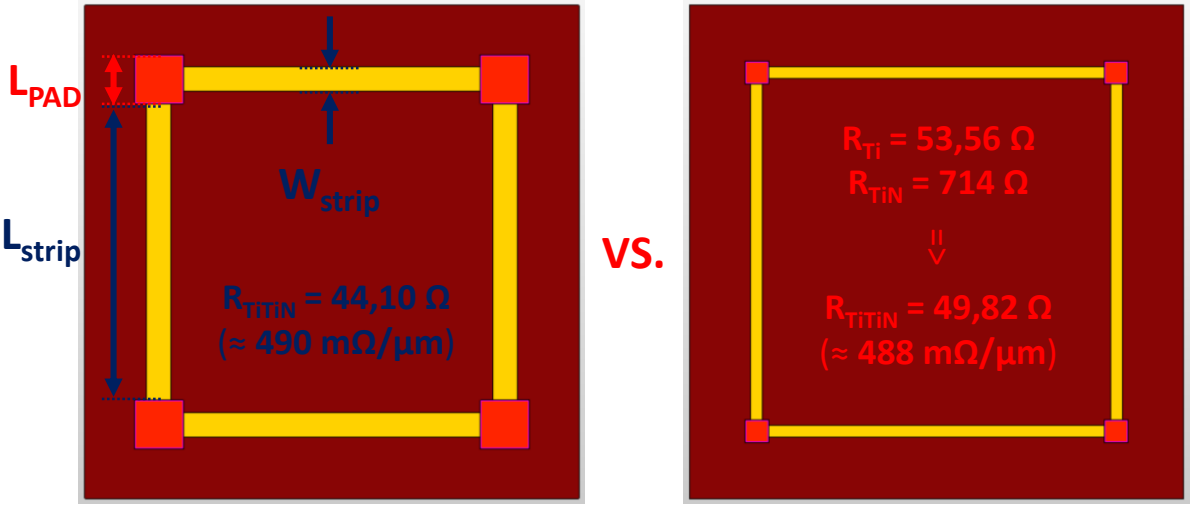

$$R = \rho \frac{L}{A} [\Omega]$$

$$A = W\ t\ [\mu m^2]$$

$$W_{strip} = \frac{L_{PAD}}{2}$$

hit 3	351.889 mesh points	273.829 mesh points
hit 8	350.489 mesh points	275.654 mesh points

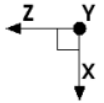

Simulated setup

✓ Electric contacts and circuit

C w Strips

L_{PAD} = 15 µm

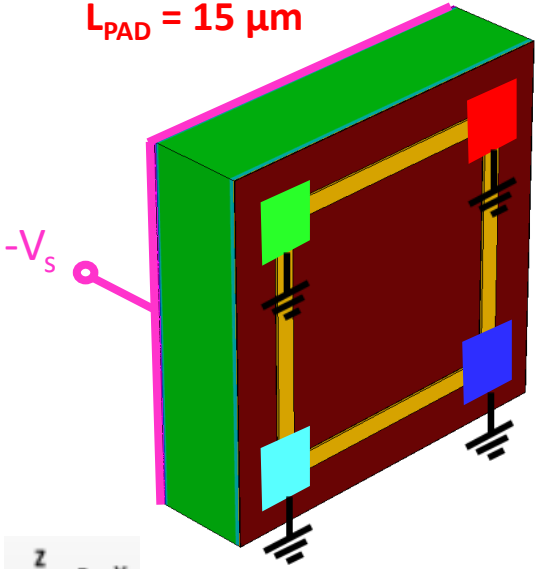

L_{PAD} = 7 µm

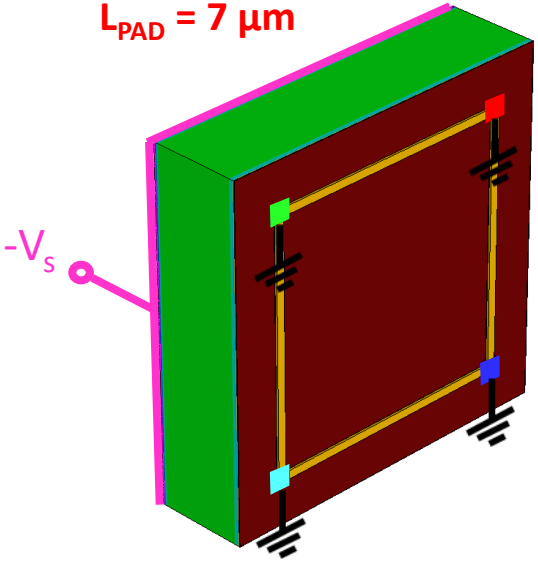

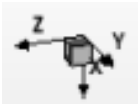

- ❑ **BACK** => $\mathbf{V_s}$ = -110 V
- ❑ **PAD1** => V_1 = 0 (**GND**)
- ❑ **PAD2** => V_2 = 0 (**GND**)
- ❑ **PAD3** => V_3 = 0 (**GND**)
- ❑ **PAD4** => V_4 = 0 (**GND**)

Reconstruction (1/2)

✓ The position is reconstructed using the **CHARGE imbalance**

$$x_i = \frac{Q_{top\,right} + Q_{bottom\,right} - Q_{top\,left} - Q_{bottom\,left}}{Q_{tot}}$$

$$z_i = \frac{Q_{top\,right} + Q_{top\,left} - Q_{bottom\,left} - Q_{bottom\,right}}{Q_{tot}}$$

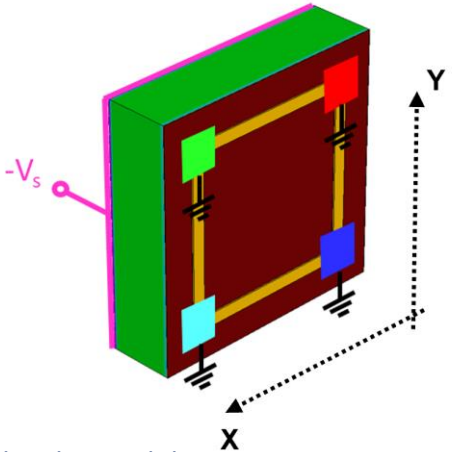

Pad Length = 15 µm

Pitch = 105 µm

@ V_{Back} = -110 V

1 MIP

$R_{s,n++} \approx 721\ \Omega_{sq}$

$R_{TiTiN} \approx 490\ m\Omega/\mu m$

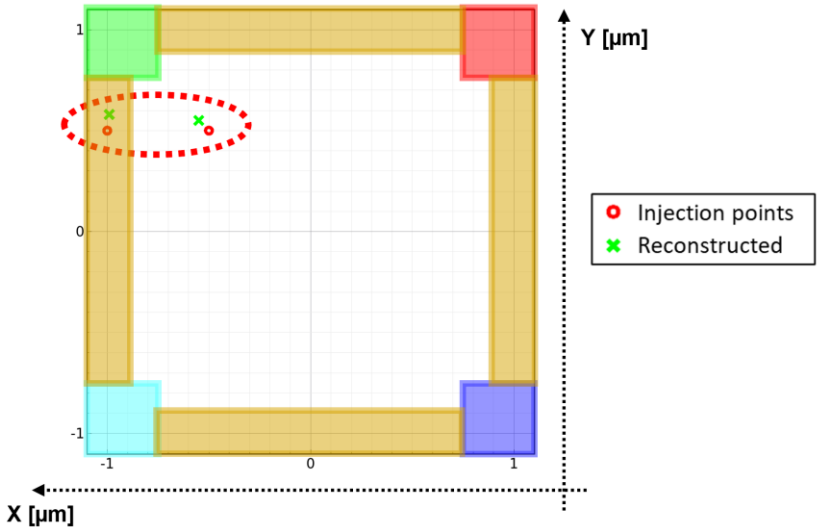

Results from *TCAD* simulations

Avalanche model: **Massey**. Temperature **300 K**

Reconstruction (2/2)

✓ The position is reconstructed using the **CHARGE imbalance**

$$x_i = \frac{Q_{top\,right} + Q_{bottom\,right} - Q_{top\,left} - Q_{bottom\,left}}{Q_{tot}}$$

$$z_i = \frac{Q_{top\,right} + Q_{top\,left} - Q_{bottom\,left} - Q_{bottom\,right}}{Q_{tot}}$$

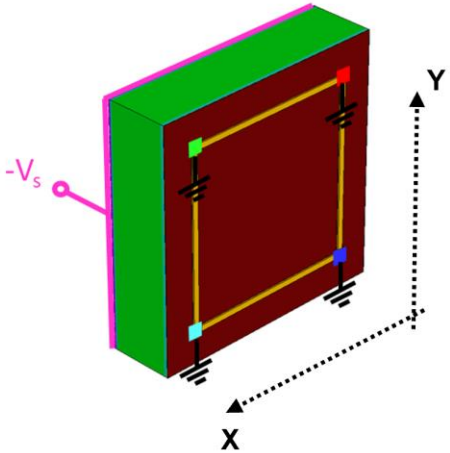

Pad Length = 7 µm

Pitch = 109 µm

@ V_{Back} = -110 V

1 MIP

$R_{s,n++} \approx 721\ \Omega_{sq}$

$R_{TiTiN} \approx 488\ m\Omega/\mu m$

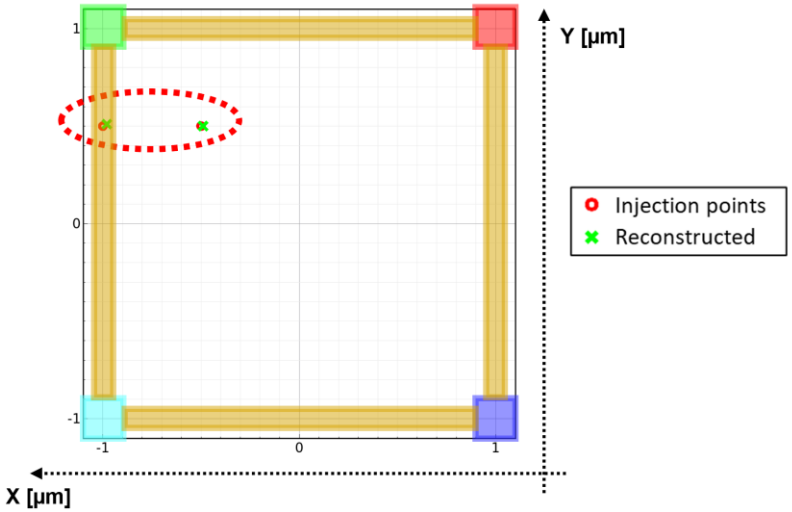

Results from *TCAD* simulations

Avalanche model: **Massey**. Temperature **300 K**

Conclusions

- ✓ **Strategy** for TCAD numerical simulation of LGAD devices.
- ✓ **Results** obtained under **different operating conditions** (device biasing, fluence).
- ✓ **Good agreement** between simulation predictions and experimental data **for both non-irradiated and irradiated** LGAD device.
- ✓ **Combination** of "New University of Perugia TCAD model" and the "acceptor removal" analytical model is used to simulate the **radiation damage effects**

  => successful **description** of the **decrease in gain with** an increase in **fluence**.
- ✓ **Application** of the validated simulation framework for the analysis of **different innovative options in particular Compensated and RSD LGAD=> optimization** for their **use in the future HEP experiments**.
- ✓ **Ongoing comparison** between **simulation findings** and **new experimental data** of real devices

  => new guidelines for **future production** of **radiation-resistant LGADs**.

BACKUP SLIDES

Low-Gain Avalanche Diodes (LGADs)

- Most promising devices to cope with the high spatial density of particles hits due to the increasing radiation fluence expected in the HL-LHC at CERN.
- **LGAD structure**: pin diode with the additional inclusion of a p+-type layer just below the n-contact, which is commonly called *multiplication layer.*
- By applying a reverse-bias, this layer is responsible for a **multiplication of carriers**.

$$G_{aval} = \boldsymbol{\alpha_n} n v_n + \boldsymbol{\alpha_p} p v_p \qquad \boldsymbol{\alpha} = \frac{E}{E_{th}} e^{-\frac{E_i}{E}}$$

- By accurately chosing the **peak and shape of the implanted p+ profile**, it is possible to control the **avalanche mechanism** in order to obtain the required internal gain with a sufficiently high breakdown voltage.
- One of the best tools **for predicting the behaviour of the avalanche process** is **device-level simulation**

Technology-CAD simulations

- **TCAD simulation tools** solve fundamental, physical partial differential equations, such as diffusion and transport equation for discretized geometries (finite element meshing).
- This deep physical approach gives TCAD simulation **predictive accuracy**.
- **Synopsys© Sentaurus TCAD**

$$\begin{cases} \nabla \cdot (-\varepsilon_s \nabla \phi) = q \ \ (N_D^+ - N_A^- + p - n) & \text{Poisson} \\ \dfrac{\partial n}{\partial t} - \dfrac{1}{q} \nabla \cdot \vec{J}_n = U_n & \text{Electron continuity} \\ \dfrac{\partial p}{\partial t} + \dfrac{1}{q} \nabla \cdot \vec{J}_p = U_p & \text{Hole continuity} \end{cases}$$

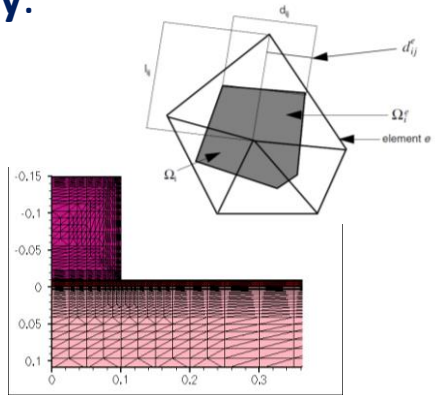

$\vec{J}_n, \vec{J}_p$

$$U_{n,p} = G - R$$

Radiation damage effects (1/2)

- ✓ in **silicon sensors**

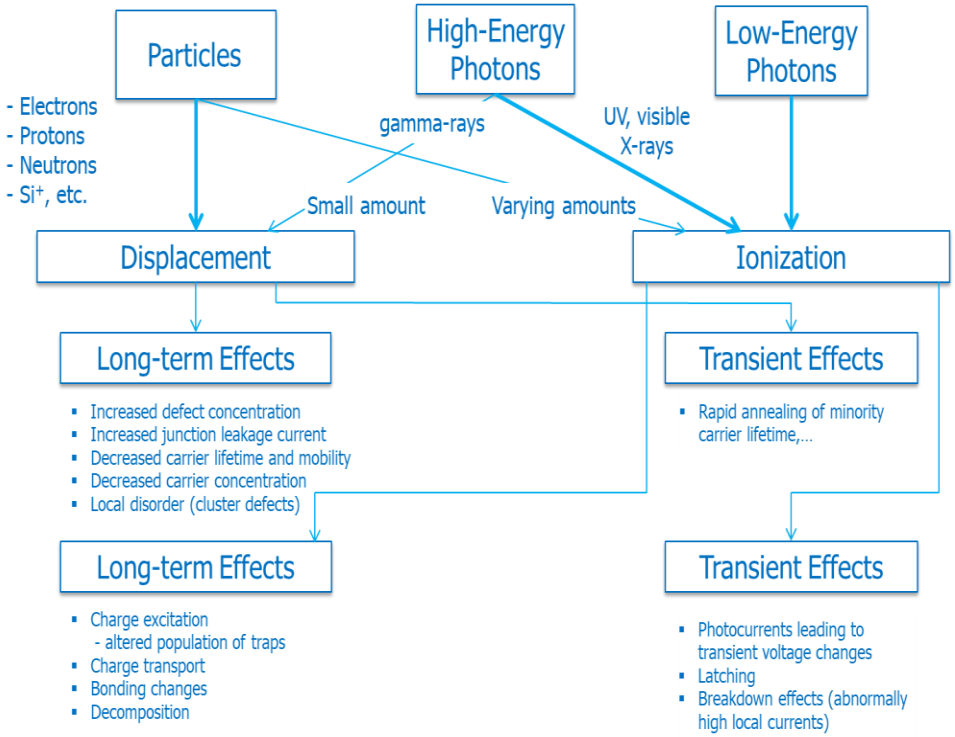

Two main **types of radiation damage** in detectors materials:

- ➢ **SURFACE damage** => Ionization
  - ✓ Build-up of trapped charge within the oxide;
  - ✓ Bulk oxide traps increase;
  - ✓ Interface traps increase;
  - ✓ Q_{ox}, N_{IT}.
- ➢ **BULK damage** => Atomic displacement
  - ✓ Silicon lattice defect generations;
  - ✓ Point and cluster defects;
  - ✓ Deep-level trap states increase;
  - ✓ Change of effective doping concentration;
  - ✓ N_T.

Radiation damage effects (2/2)

- ✓ in **LGAD devices**

- **Acceptor removal mechanism**[1]: the active (substitutionals) doping elements are partially removed from their lattice sites due to the ionizing radiation and then de-activated after a kick-out reaction (Watkins mechanism[2]) that produces ion-acceptor complexes (interstitials)
- Transformation of electrically active acceptors into defect complexes that no longer have dopant properties
- This has been recently suggested as a possible explanation for the significant degradation of gain (charge multiplication) observed on LGAD devices after irradiation.

[1] G. Kramberger, M. Baselga et al., J. Inst., vol. 10, no. 7, p. P07006, 2015
[2] G. D. Watkins, *Defects and Their Structure in Non-metallic Solids*, B. Henderson and A. E. Hughes, Eds. New York: Plenum, 1975

TCAD radiation damage models used

- **"New University of Perugia model"**
  - ✓ **Combined surface and bulk** TCAD damage modelling scheme[3]
  - ✓ Traps generation mechanism
- **Acceptor removal mechanism**

$$N_{GL}(\phi) = NA(0)e^{-c\phi}$$

where

- **G**ain **L**ayer (**GL**)
- **c**, removal rate, evaluated using the **Torino parameterization**[4]

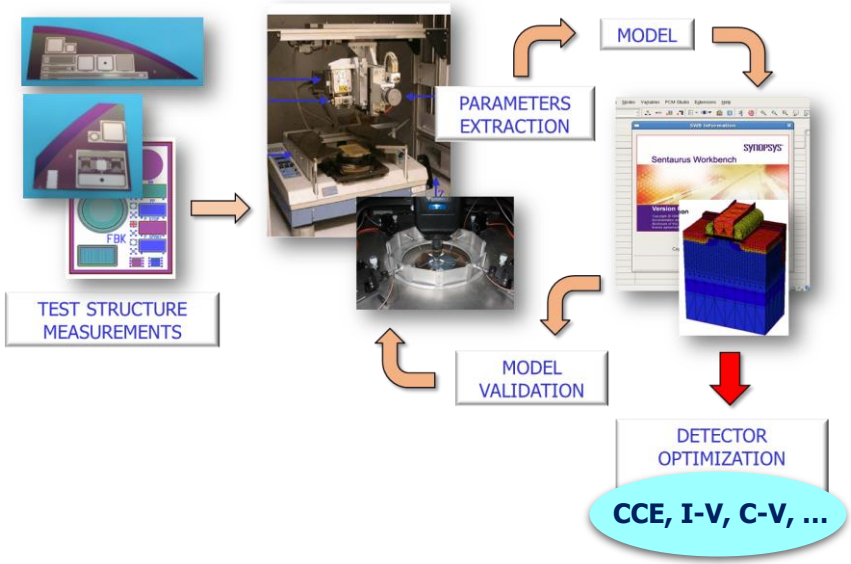

Surface damage (+ Q_{ox})

Type	Energy (eV)	Band width (eV)	Conc. (cm^{-2})
Acceptor	$E_C \le E_T \le E_C$-0.56	0.56	$D_{IT} = D_{IT}(\Phi)$
Donor	$E_V \le E_T \le E_V$+0.6	0.60	$D_{IT} = D_{IT}(\Phi)$

Bulk damage

Type	Energy (eV)	η (cm^{-1})	σ_n (cm^2)	σ_h (cm^2)
Donor	E_C - 0.23	0.006	2.3×10^{-14}	2.3×10^{-15}
Acceptor	E_C - 0.42	1.6	1×10^{-15}	1×10^{-14}
Acceptor	E_C - 0.46	0.9	7×10^{-14}	7×10^{-13}

[3] AIDA2020 report, *TCAD radiation damage model - CERN Document Server*
[4] M. Ferrero et al., *Radiation resistant LGAD design*, Nucl. Inst. And Meth. In Phys. Res. A, November 30, 2018.

Methodology

DC / AC analysis → Transient analysis → Gain calculation

- **DC biasing (static)**
  - n cathode: 0 V
  - p anode: *sweep*
    - ✓ start = 0 V
    - ✓ step = - 25 V (from 100 V)
    - ✓ stop = - 1000 V
  - Temperature
    - ✓ 300 K for not irr., 253 K for irr. [7]
- **AC biasing (small-signal)**
  - For each DC bias step, superimposition of a 1 V_{pp}, 1 kHz sinusoid
  - Impedance matrix for each node of the discretized grid
  - Temperature 300 K for not irr. / irr.

- For each DC bias step, one **Time-Variant (TV)** simulation of impinging particle (**MIP**), following the **"HeavyIon" model**
  - instant of penetration 1 ns
  - through the whole device
  - Linear Energy Transfer (LET)

$$LET_f = \frac{E_{LOSS}}{E} \quad \frac{pC}{\mu m}$$

where

$$E = 3{,}68 \ eV$$

[5] $$E_{LOSS} = 0{,}027\, log(y) + 0{,}126 \quad \frac{keV}{\mu m}$$

- Leakage current calculation
  - instant = 0,9 ns
- Leakage current offset subtracted from the simulated I(t) curve
- Calculation of **Collected Charge (CC)** as the **integral of the current**

$$Gain = \frac{CC_{LGAD}}{CC_{PIN}}$$ [6]

[5] S. Meroli et al., *Energy loss measurement for charged particles in very thin silicon layers*, JINST 6 P06013, 2011
[6] V. Sola et al., *First FBK production of 50 µm ultra-fast silicon detectors*, Nucl. Instrum. Methods Phys. Res. A, 2019
[7] A. Chilingarov, *Temperature dependence of the current generated in si bulk*, JINST 8 P10003, 2013.

Transient responce: “HeavyIon” model

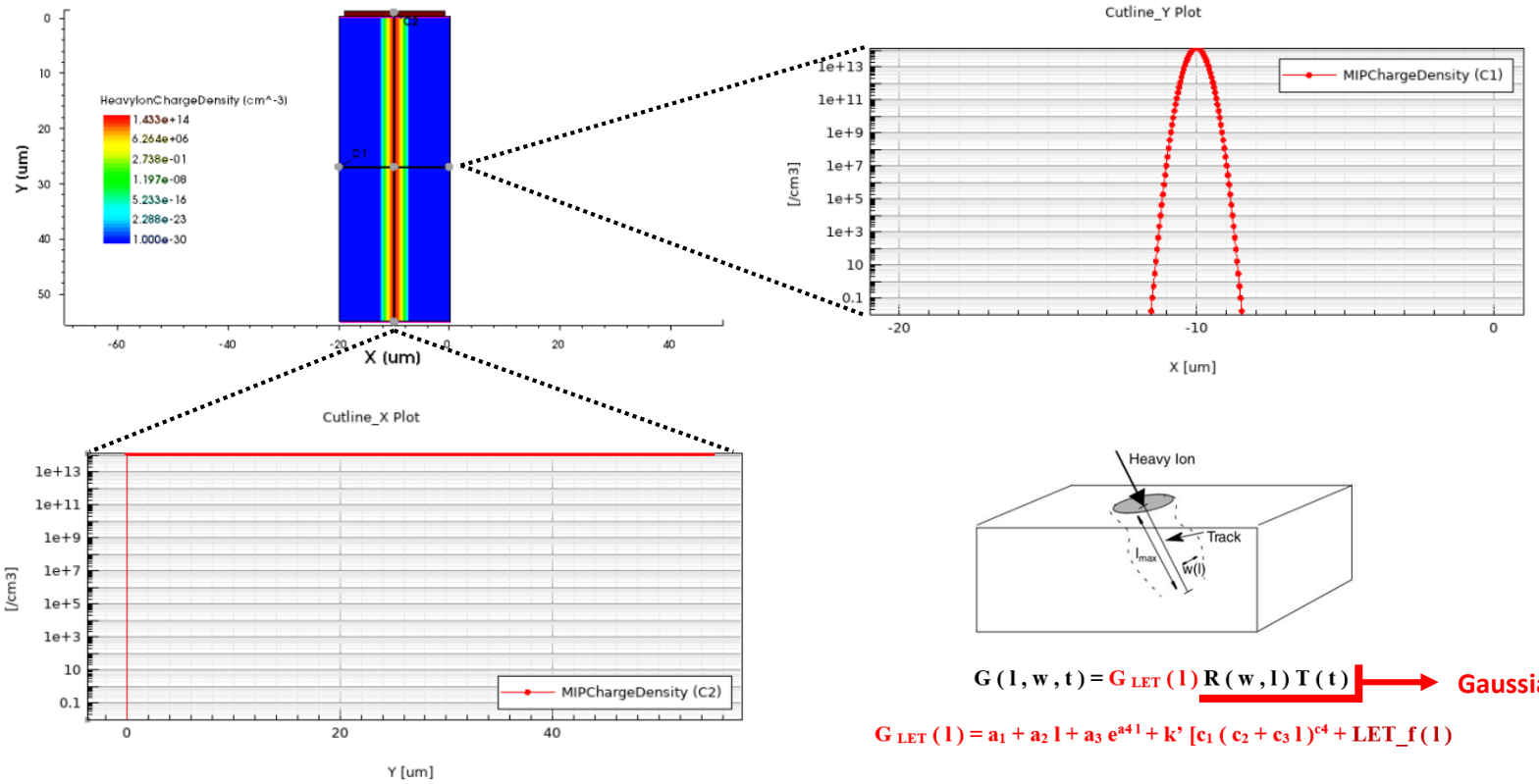

$$G(l, w, t) = G_{LET}(l)\, R(w, l)\, T(t) \rightarrow \text{Gaussian}$$

$$G_{LET}(l) = a_1 + a_2 l + a_3 e^{a4\, l} + k' [c_1 (c_2 + c_3 l)^{c4} + LET\_f(l)$$

Pre-Irradiation: Experimental Data (FBK UFSD2 Production)

Gain Measurement – Φ=0

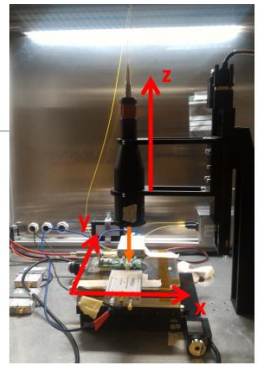

TCT Setup from Particulars
Pico-second IR laser at 1064 nm
Laser spot diameter ~ 50 µm
Cividec Broadband Amplifier (40dB)
Oscilloscope Lecroy 640Zi
Room temperature
Laser attenutation 82% (3 MIP 150 fC)

LD peak: 6.1E16/cm³ => 6.4E16/cm³ (*)
HD peak: 4.0E16/cm³

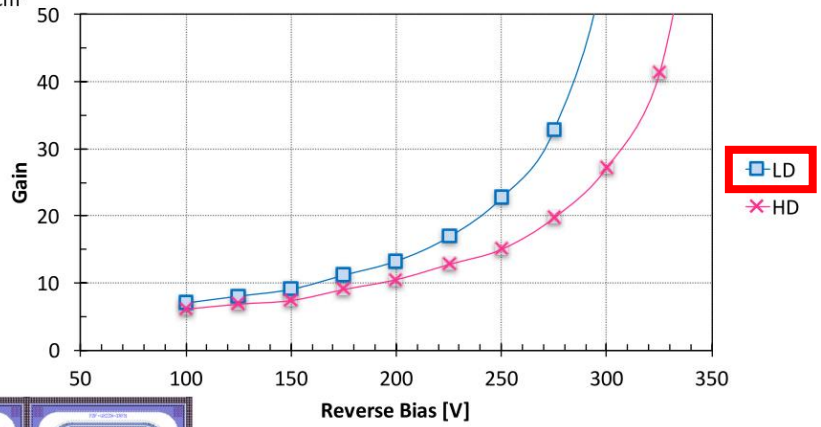

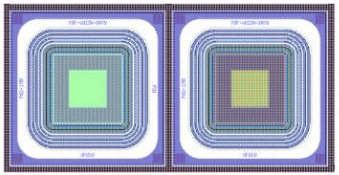

GAIN = Charge LGAD / Charge PiN

	W1	W8
Bias [V]	Gain LD	Gain HD
100	7.1	6.1
125	8.1	6.9
150	9.1	7.4
175	11.2	9.1
200	13.3	10.5
225	16.9	12.8
250	22.7	15.1
275	32.8	19.8
300	61.8	27.2
325	248.8	41.3
350	-	82.3

(*) values updated to the latest measurements – V. Sola, 20/10

Post-Irradiation: Experimental Data (FBK UFSD2 Production)

Gain Measurement – Irradiated LD

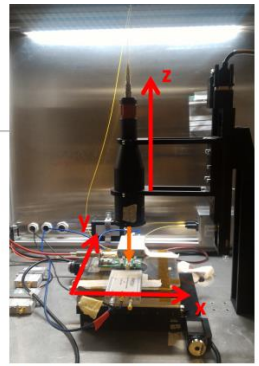

TCT Setup from Particulars
Pico-second IR laser at 1064 nm
Laser spot diameter ~ 50 µm
Cividec Broadband Amplifier (40dB)
Oscilloscope Lecroy 640Zi
Room temperature
Laser attenutation 82% (3 MIP 150 fC)

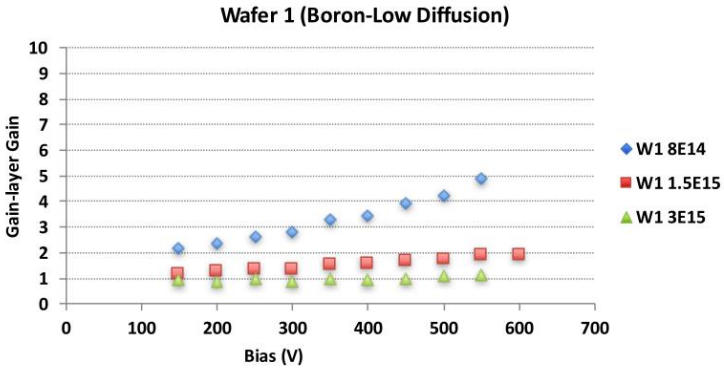

GAIN = Charge LGAD / Charge PiN irradiated at the same fluence
→ gain from gain layer only

c_{LD} = 3.85E-16 cm^2

W1

Bias [V]	Gain	
	Φ=8E14	Φ=1.5E15
150	2.1	1.14
200	2.4	1.26
250	2.7	1.36
300	2.8	1.37
350	3.3	1.52
400	3.4	1.54
450	3.9	1.65
500	4.2	1.74
550	4.9	1.87
600	-	1.90

Gain calculation (3D)

✓ **Fully-3D** structure

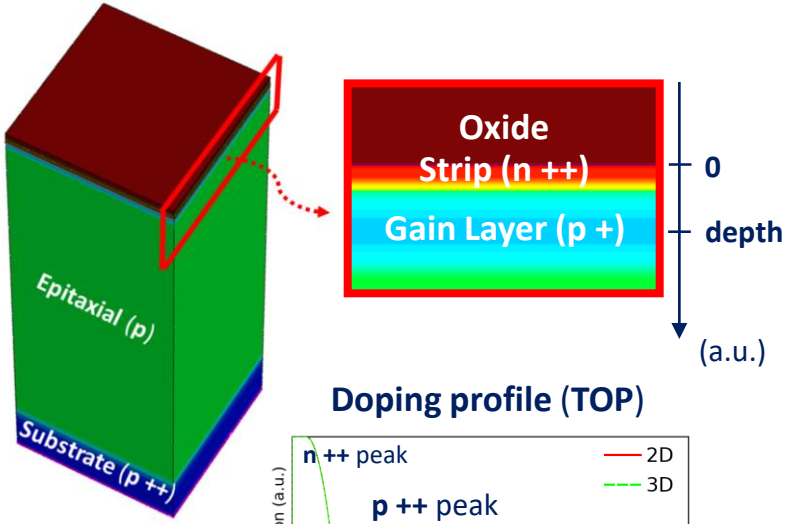

Gaussian Gain Layer **profile**

Doping profile (TOP)

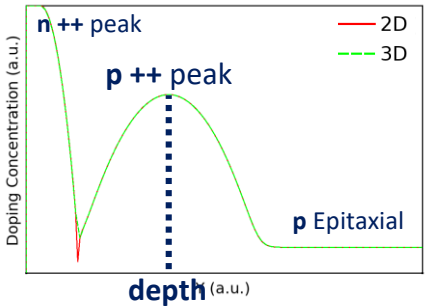

I-V, before irradiation

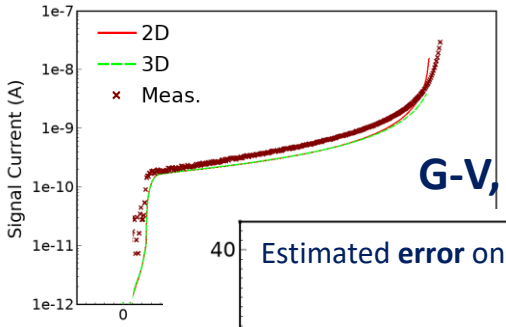

Good agreement!

G-V, before irradiation

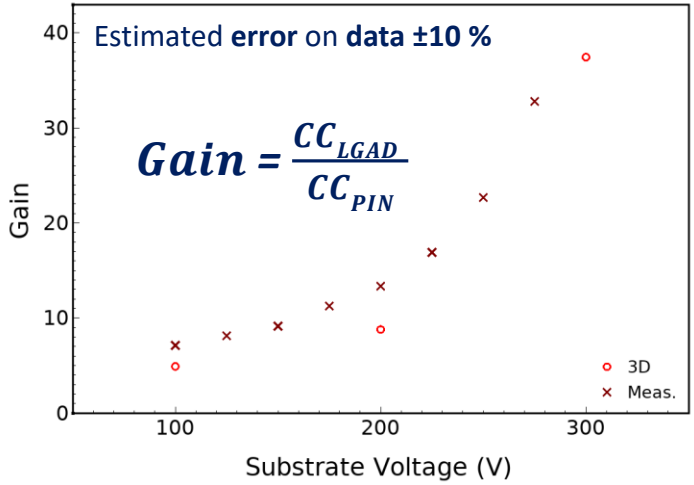

Avalanche model: **Massey**. Temp. **300 K**. Electrical contact area **1mm²**

Gain calculation

✓ **Simulation** results, **before** and **after irradiation** (fluences **1.0e16** and **5.0e16 n_{eq}/cm^2**)

G-V, before irradiation

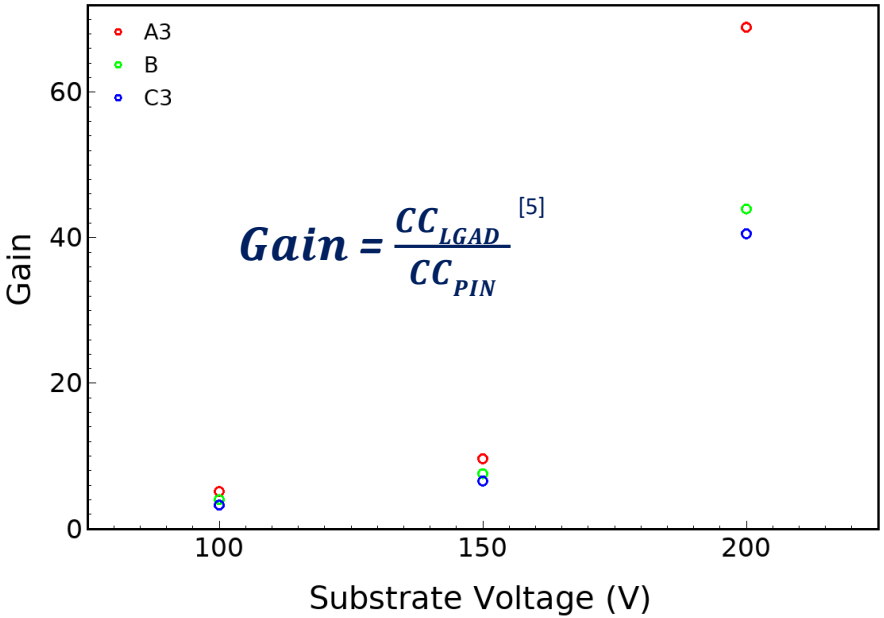

G-V, after irradiation

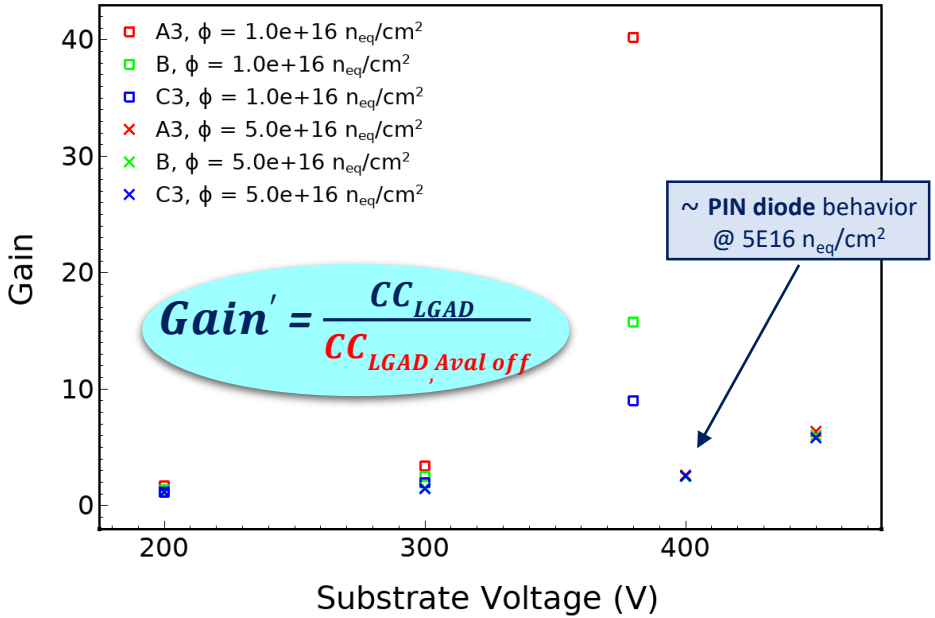

Avalanche model: **Massey**. Temperature **300 K**

[5] V. Sola et al., *First FBK production of 50 µm ultra-fast silicon detectors*, Nucl. Instrum. Methods Phys. Res. A, 2019.

Simulated setup (2/2)

✓ Electric contacts and circuit

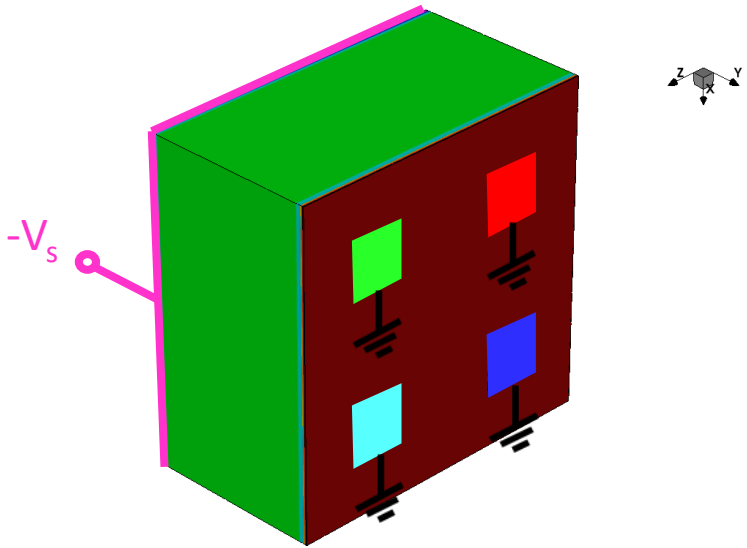

- **BACK** => **$-V_s$**: 0 – 1000 V
- **PAD1** => V_1 = 0 (**GND**)
- **PAD2** => V_2 = 0 (**GND**)
- **PAD3** => V_3 = 0 (**GND**)
- **PAD4** => V_4 = 0 (**GND**)

Reconstruction (3/3)

Results from *Spice* simulations **VS.** **Results** from *TCAD* simulations

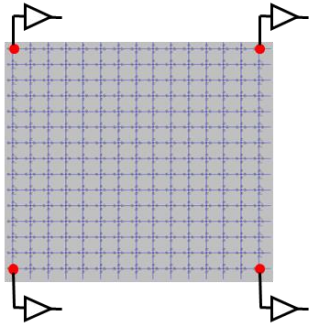

AMPLITUDE imbalance

$$x_i = \frac{A_{top\ right} + A_{bottom\ right} - A_{top\ left} - A_{bottom\ left}}{A_{tot}}$$

$$z_i = \frac{A_{top\ right} + A_{top\ left} - A_{bottom\ left} - A_{bottom\ right}}{A_{tot}}$$

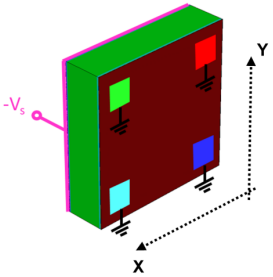

CHARGE imbalance

$$x_i = \frac{Q_{top\ right} + Q_{bottom\ right} - Q_{top\ left} - Q_{bottom\ left}}{Q_{tot}}$$

$$z_i = \frac{Q_{top\ right} + Q_{top\ left} - Q_{bottom\ left} - Q_{bottom\ right}}{Q_{tot}}$$

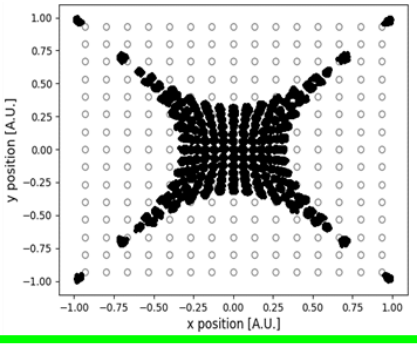

Empty circles: injection points

Filled circles: reconstructed points

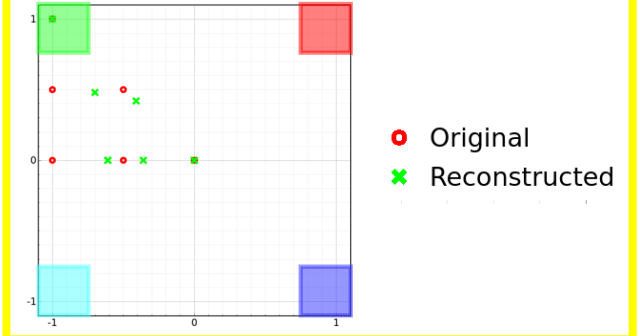

From **L. Menzio et al.**, 17th ''TREDI'' Workshop 03/03/22.

Active (TV) behavior (3/7)

- ✓ **3D** structure, **2x2 PADs**
  - **hit 3**, **1 MIP**
  - **V_s = -200 V**

@ $R_{s,n++} \approx 203\ \Omega_{sq}$

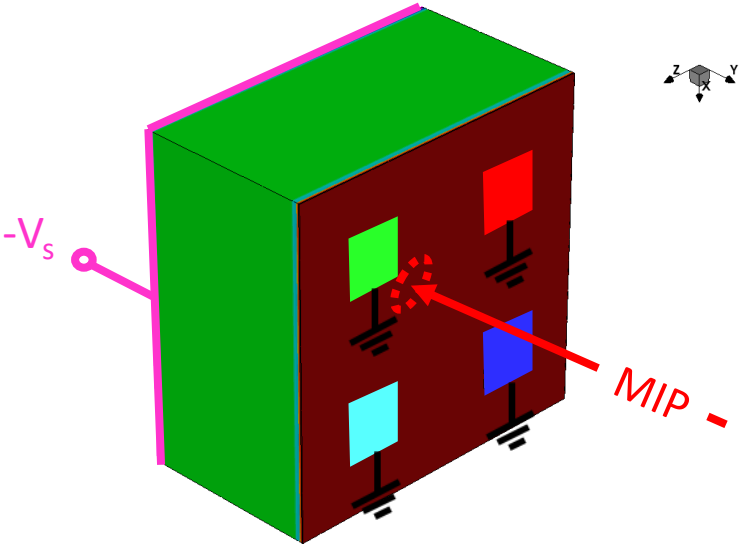

I-t, not irr.

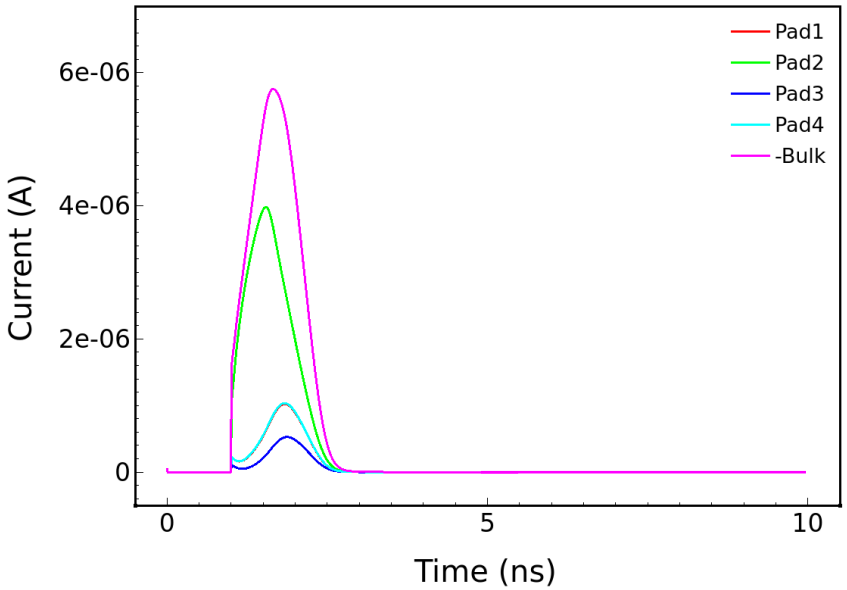

Avalanche model: **Massey**. Temperature **300 K**

Active (TV) behavior (4/7)

- ✓ **3D** structure, **2x2 PADs**
  - **hit 4**, **1 MIP**
  - V_s = **-200 V**

@ $R_{s,n++} \approx 203\ \Omega_{sq}$

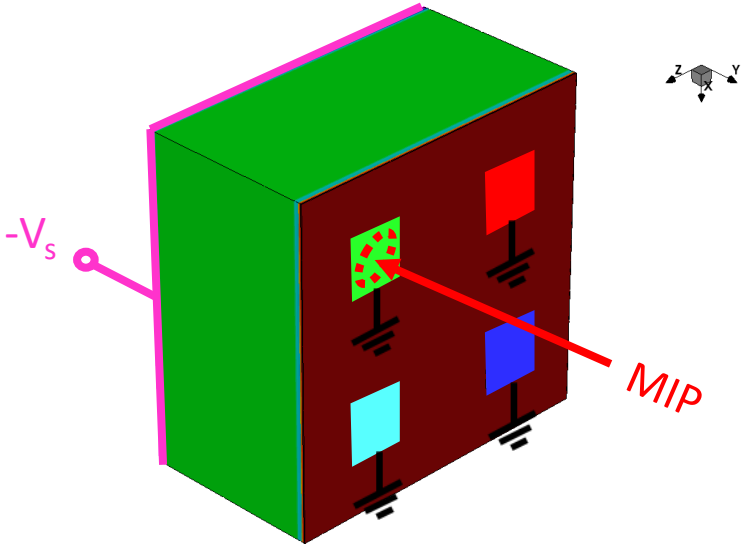

I-t, not irr.

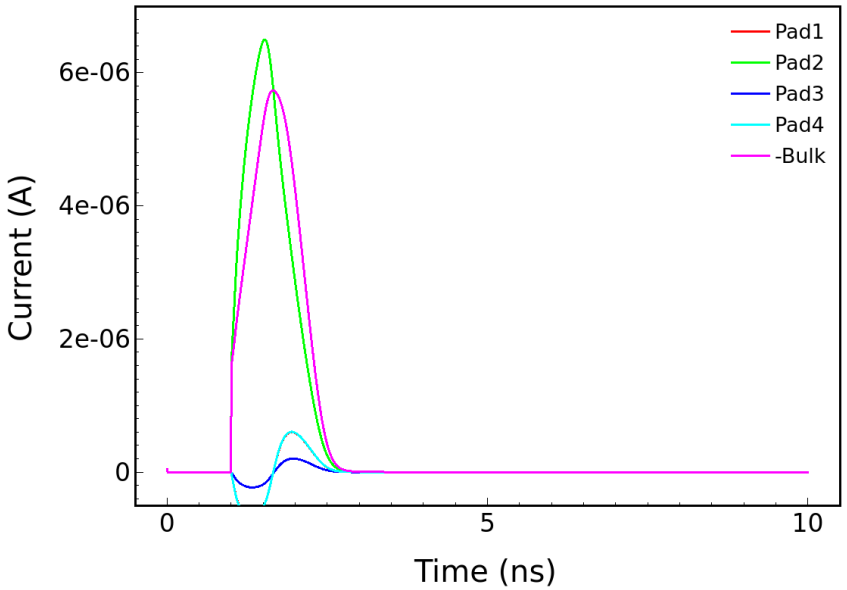

Avalanche model: **Massey**. Temperature **300 K**

Active (TV) behavior (5/7)

- ✓ **3D** structure, **2x2 PADs**
  - **hit 5**, **1 MIP**
  - V_s = **-200 V**

@ $R_{s,n++} \approx 203\ \Omega_{sq}$

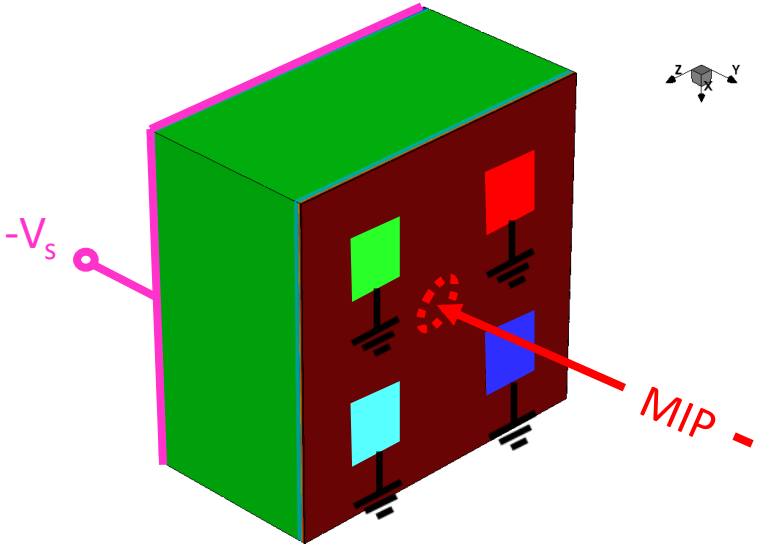

I-t, not irr.

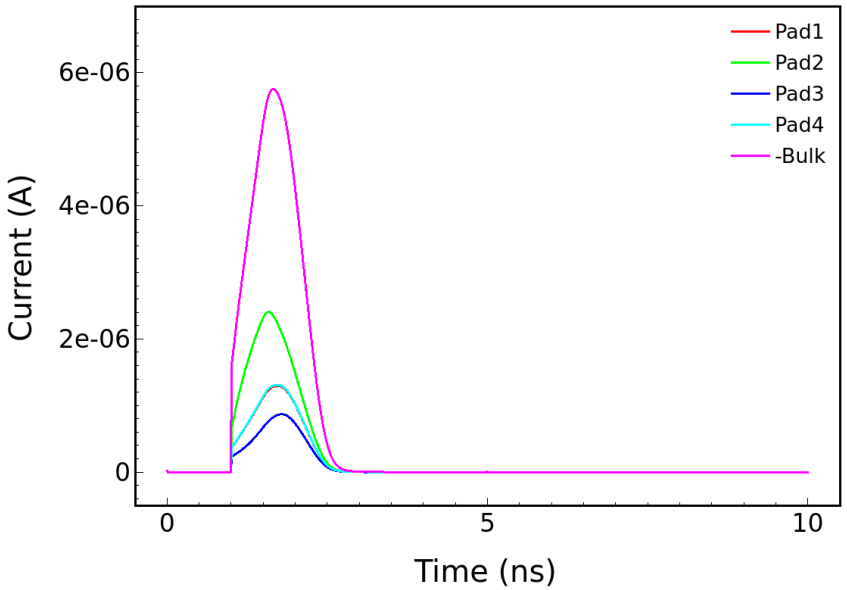

Avalanche model: **Massey**. Temperature **300 K**

Active (TV) behavior (6/7)

- ✓ **3D** structure, **2x2 PADs**
  - **hit 6**, **1 MIP**
  - V_s = **-200 V**

@ $R_{s,n++} \approx 203\ \Omega_{sq}$

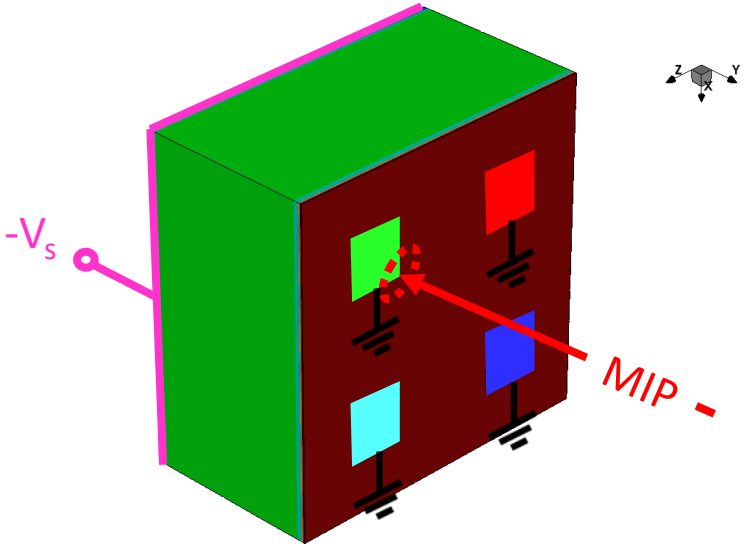

I-t, not irr.

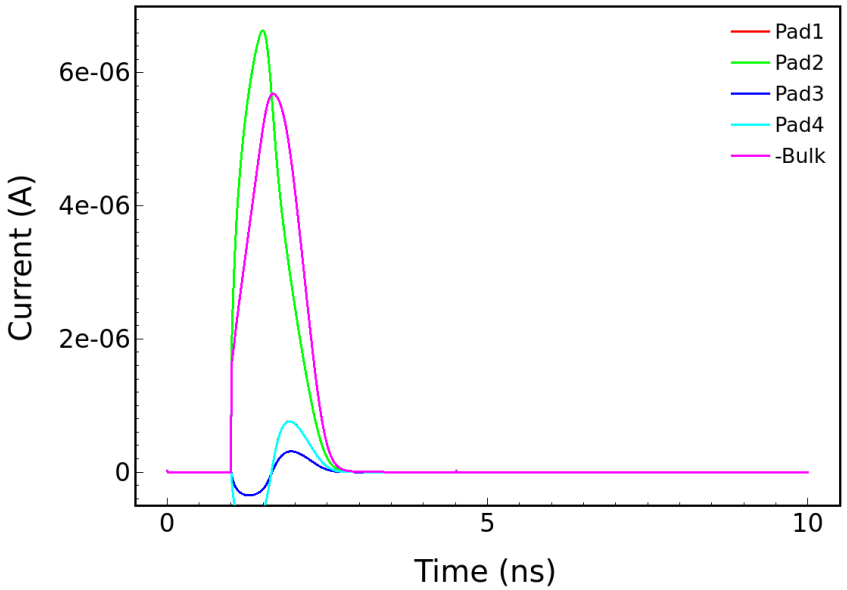

Avalanche model: **Massey**. Temperature **300 K**

Active (TV) behavior (7/7)

- ✓ **3D** structure, **2x2 PADs**
  - **hit 7**, **1 MIP**
  - **V_s = -200 V**

@ $R_{s,n++} \approx 203\ \Omega_{sq}$

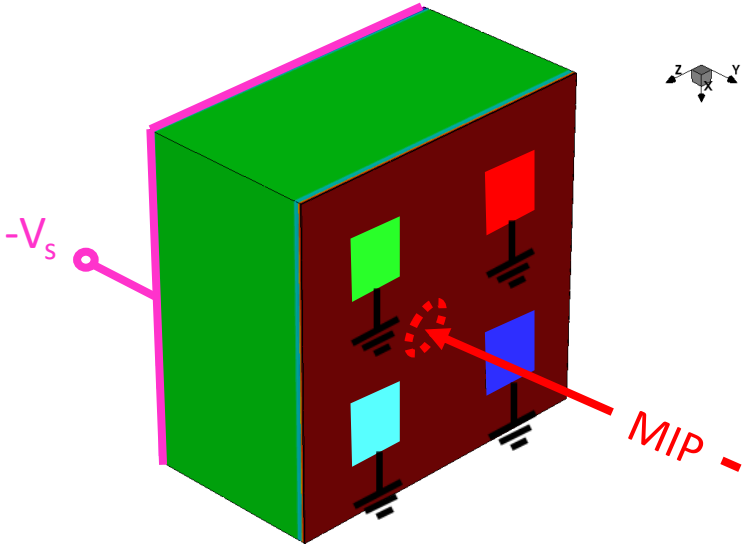

I-t, not irr.

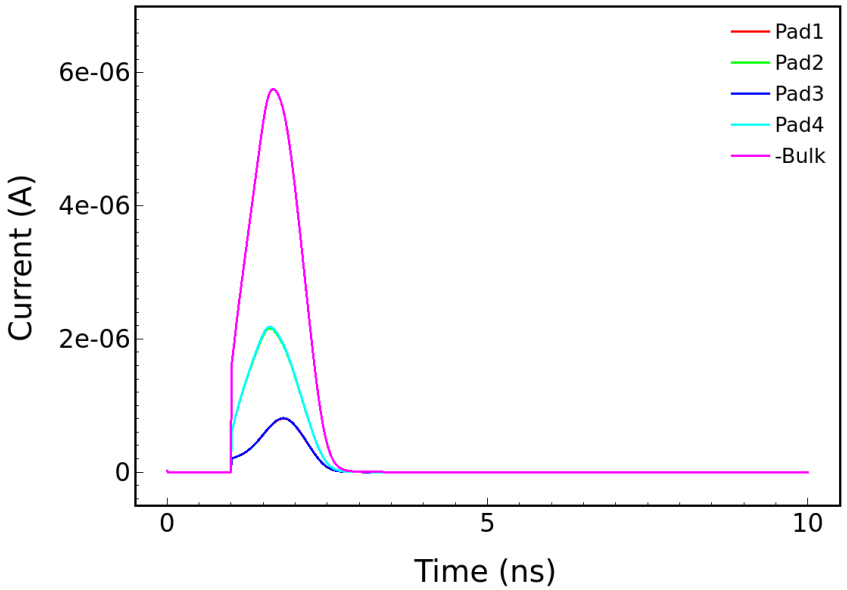

Avalanche model: **Massey**. Temperature **300 K**

Next step - Simulated setup

✓ Electric contacts and circuit

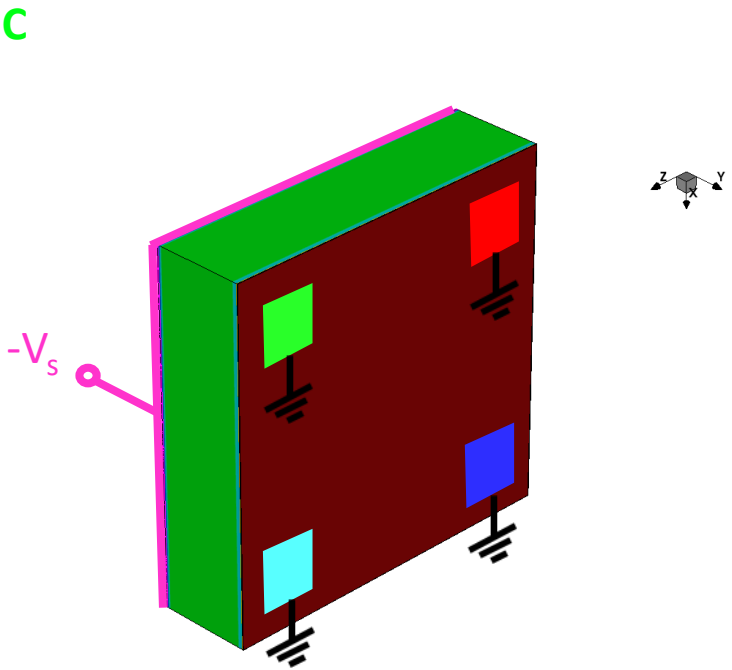

- ❑ **BACK** => $\mathbf{V_s}$ = -110 V
- ❑ **PAD1** => V_1 = 0 (**GND**)
- ❑ **PAD2** => V_2 = 0 (**GND**)
- ❑ **PAD3** => V_3 = 0 (**GND**)
- ❑ **PAD4** => V_4 = 0 (**GND**)

Active (TV) behavior (1/4)

- ✓ **3D** structure, **2x2 PADs**, **C wo Strip** (19 h 06 min, 4 lic.)
  - **hit 2**, **1 MIP**
  - **V_s = -110 V**

@ $R_{s,n++} \approx 721\ \Omega_{sq}$

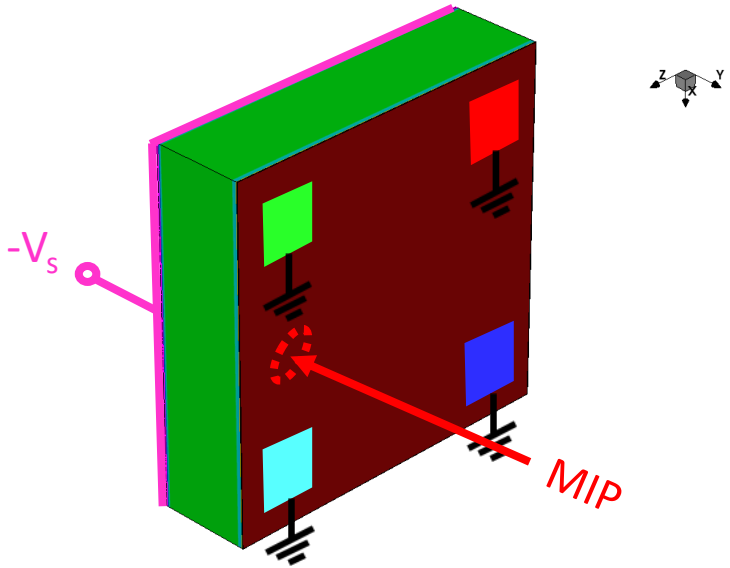

I-t, not irr.

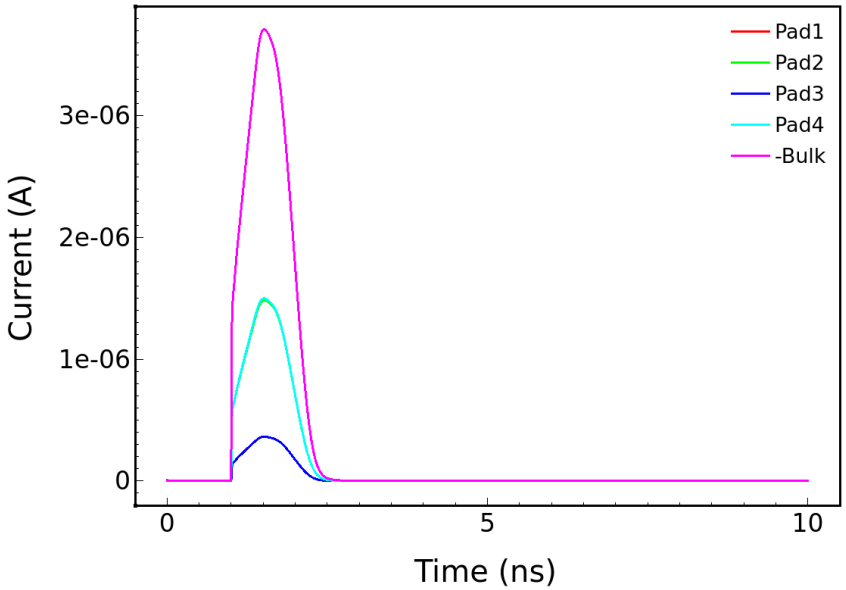

Avalanche model: **Massey**. Temperature **300 K**

Active (TV) behavior (2/4)

- ✓ **3D** structure, **2x2 PADs**, **C wo Strip** (19 h 21 min, 4 lic.)
  - **hit 3**, **1 MIP**
  - **V_s = -110 V**

@ $R_{s,n++} \approx 721\ \Omega_{sq}$

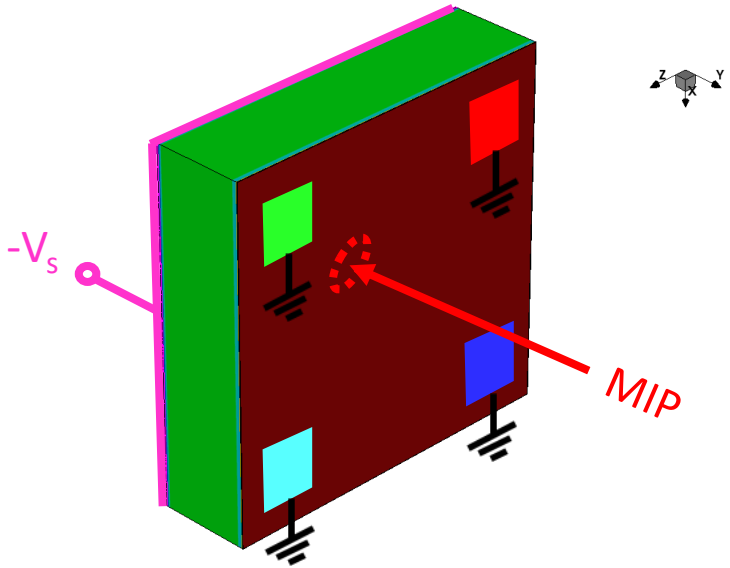

I-t, not irr.

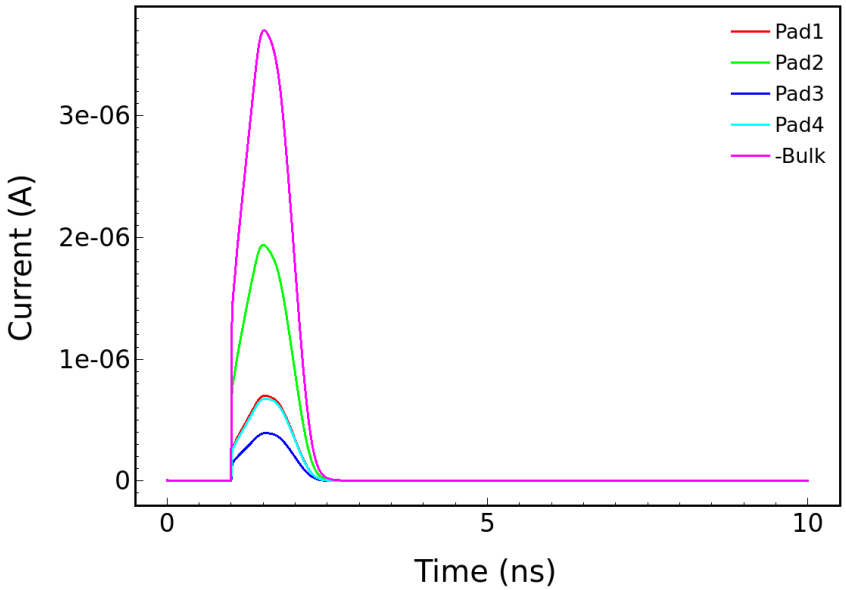

Avalanche model: **Massey**. Temperature **300 K**

Active (TV) behavior (3/4)

- ✓ **3D** structure, **2x2 PADs**, **C wo Strip** (19 h 20 min, 4 lic.)
  - **hit 7**, **1 MIP**
  - **V_s = -110 V**

@ $R_{s,n++} \approx 721\ \Omega_{sq}$

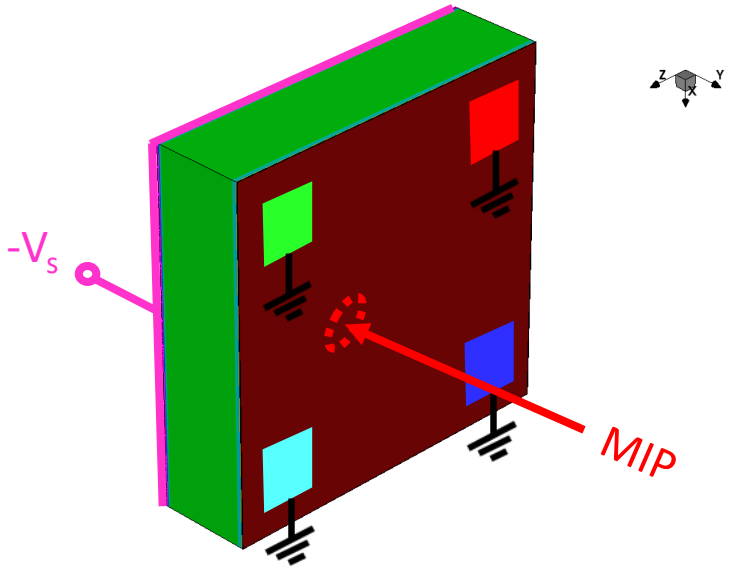

I-t, not irr.

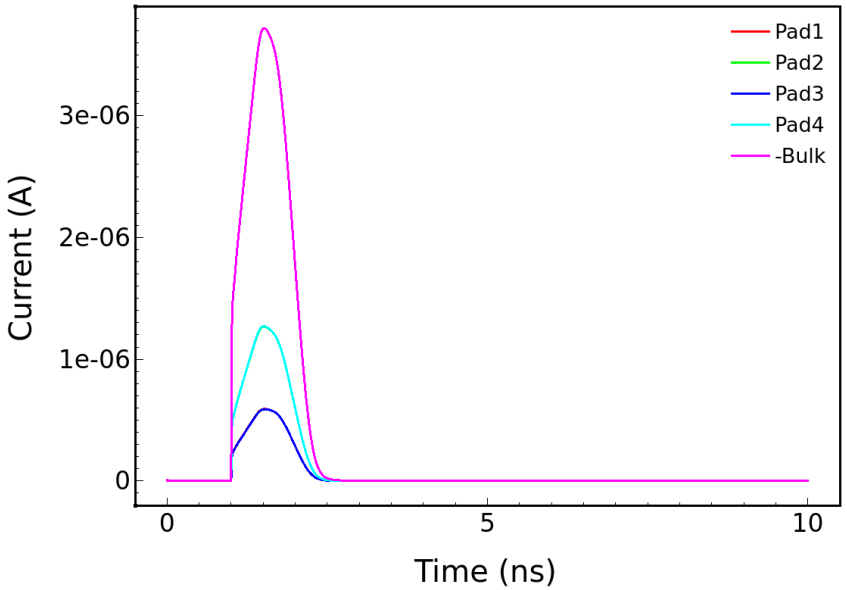

Avalanche model: **Massey**. Temperature **300 K**

Active (TV) behavior (4/4)

- ✓ **3D** structure, **2x2 PADs**, **C wo Strip** (18 h 42 min, 4 lic.)
  - **hit 8**, **1 MIP**
  - **V_s = -110 V**

@ $R_{s,n++} \approx 721\ \Omega_{sq}$

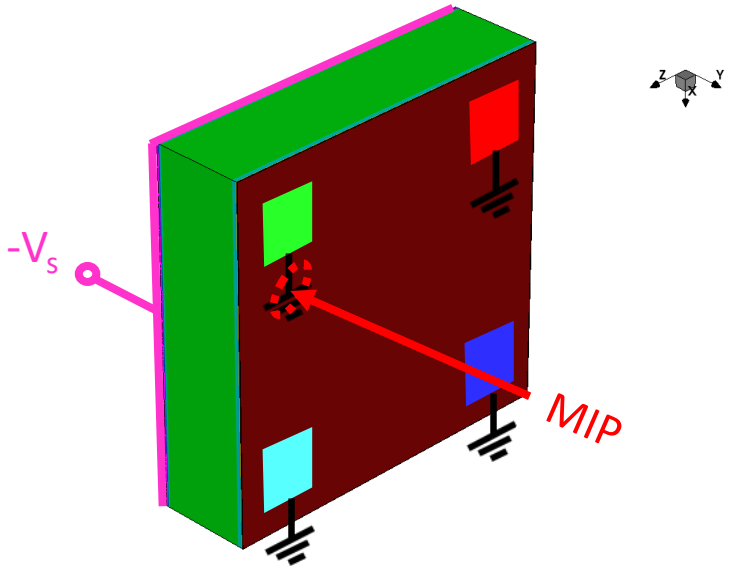

I-t, not irr.

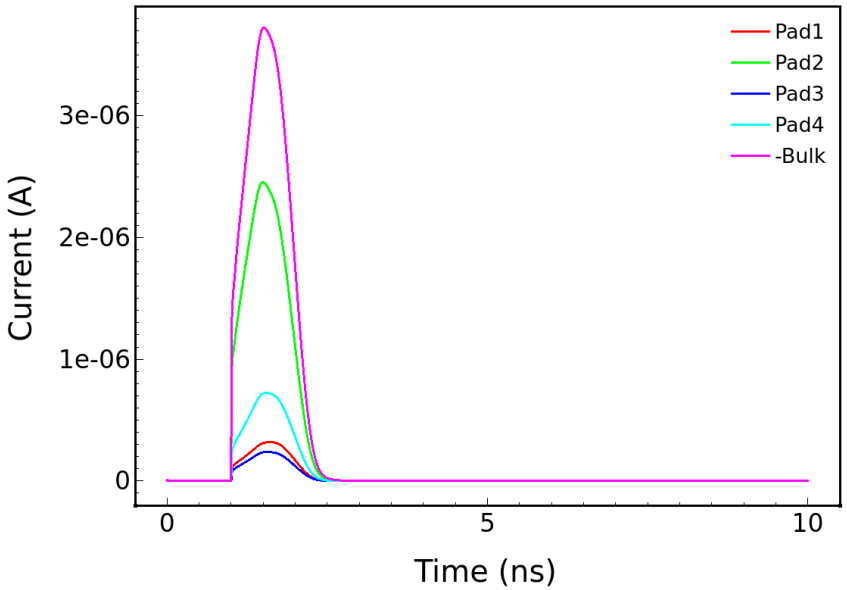

Avalanche model: **Massey**. Temperature **300 K**

Active (TV) behavior

- ✓ **3D** structure, **2x2 PADs**, **C w Strip** (30 h 38 min, 8 lic.) **@ $R_{s,n++} \approx 721\ \Omega_{sq}$**
  - **hit 3**, **1 MIP**
  - **V_s = -110 V**

L_{PAD} = 15 µm ····· **L_{PAD} = 7 µm** ——

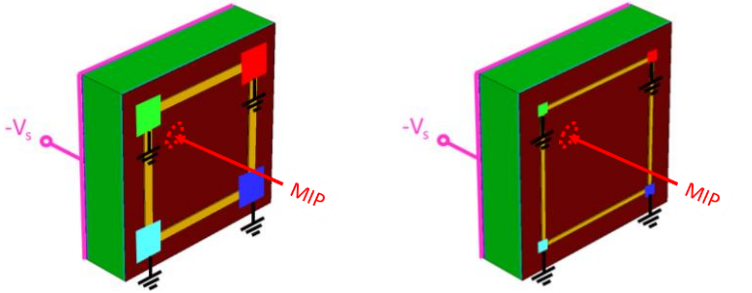

R_{TiTiN} = 44,10 Ω
(≈ 490 mΩ/µm)

R_{TiTiN} = 49,82 Ω
(≈ 488 mΩ/µm)

I-t, not irr.

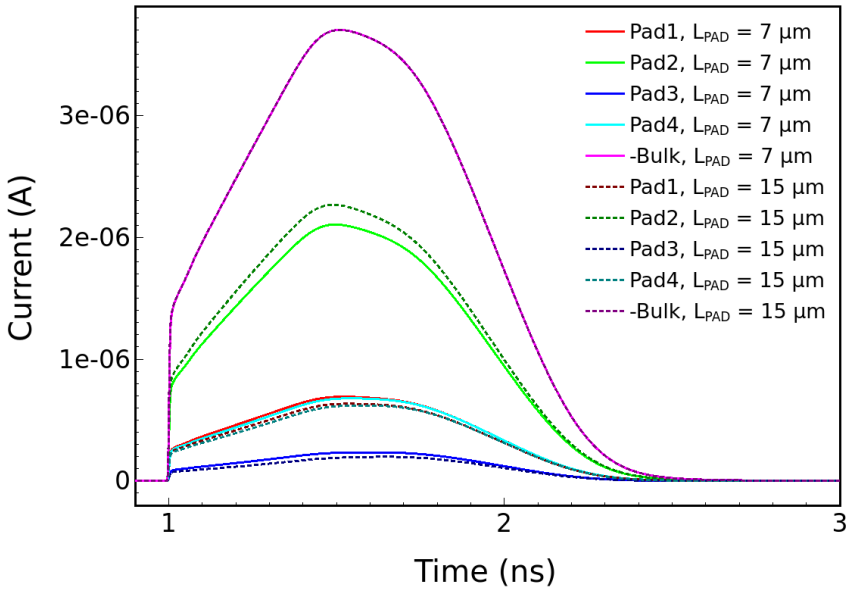

Avalanche model: **Massey**. Temperature **300 K**

Active (TV) behavior

- ✓ **3D** structure, **2x2 PADs**, **C w Strip** (31 h 24 min, 8 lic.) **@ $R_{s,n++} \approx 721\ \Omega_{sq}$**
  - **hit 8**, **1 MIP**
  - **V_s = -110 V**

L_{PAD} = 15 µm ····· **L_{PAD} = 7 µm** ——

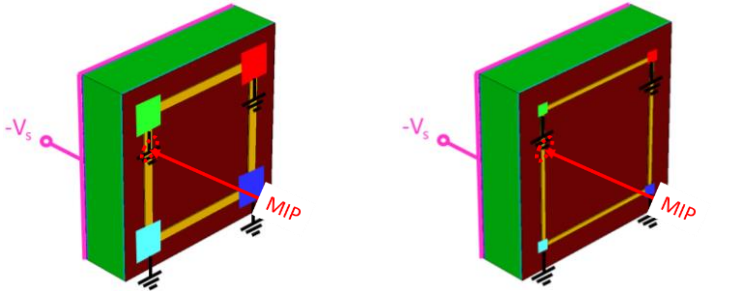

R_{TiTiN} = 44,10 Ω
(≈ 490 mΩ/µm)

R_{TiTiN} = 49,82 Ω
(≈ 488 mΩ/µm)

I-t, not irr.

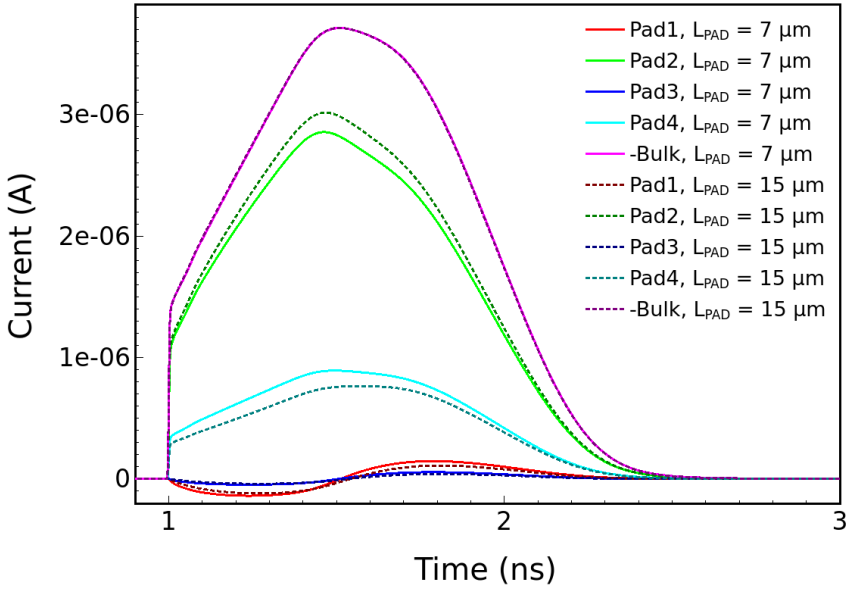

Avalanche model: **Massey**. Temperature **300 K**

Donor removal characterization

A production batch is needed to study the donor removal coefficient, c_D

Donor removal has been studied for doping densities of $10^{12} – 10^{14}$ atoms/cm^3 [M.Moll et al.]

We need to study donor removal in a range $10^{16} – 10^{18}$ atoms/cm^3

NB: Oxygen has for donor removal a very similar effect of Carbon to acceptor removal

p-in-n LGAD

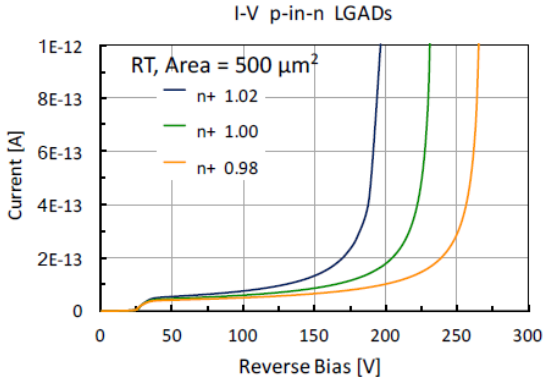

Simulation of the p-in-n LGAD parameters is in progress

→ **The main goal of the p-in-n LGAD production is to study the c_D evolution and its interplay with Oxygen co-implantation**

Next steps for DC-RSD

- ✓ **Identify the combinations of parameters** to reach the best performance.
  - ✓ Sheet resistance of the n^{++} layer
  - ✓ Sheet resistance of the resistors between read-out electrodes
  - ✓ Pitch, pad size and its geometry
- ✓ **The "New Univ. of Perugia TCAD model",** which accounts for the bulk and surface radiation damage effects on silicon detectors, **will be implemented** to predict the RSDs electrical behavior after irradiation
- ✓ **Manufacturing of the first DC-RSD production**
- ✓ **Validate and fine-tune the modeling** used in the DC-RSD simulation, based on DC-RSD run 1.

Reconstruction (2/2)

✓ The position is reconstructed using the **CHARGE imbalance**

$$x_i = \frac{Q_{top\,right} + Q_{bottom\,right} - Q_{top\,left} - Q_{bottom\,left}}{Q_{tot}}$$

$$z_i = \frac{Q_{top\,right} + Q_{top\,left} - Q_{bottom\,left} - Q_{bottom\,right}}{Q_{tot}}$$

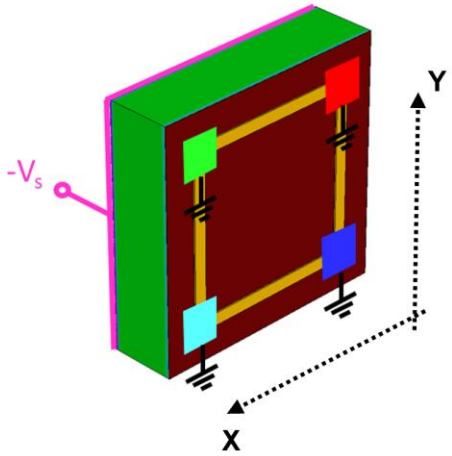

Pad Length = 15 µm

Pitch = 105 µm

@ V_{Back} = -110 V

1 MIP

$R_{s,n++} \approx 721\ \Omega_{sq}$

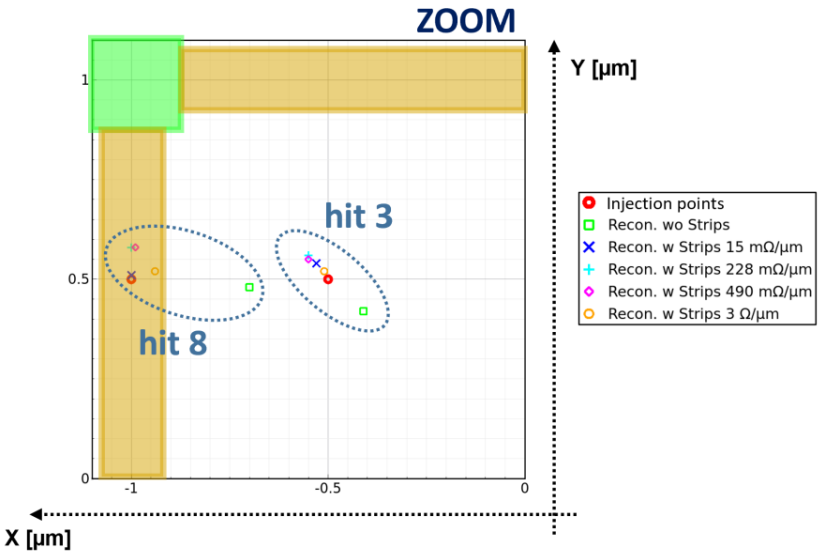

Results from *TCAD* simulations

Avalanche model: **Massey**. Temperature **300 K**